

Electronic Structure and Quadratic Hyperpolarizabilities in Organotransition-Metal Chromophores Having Weakly Coupled π -Networks. Unusual Mechanisms for Second-Order Response

David R. Kanis, Pascal G. Lacroix, Mark A. Ratner,* and Tobin J. Marks*

Contribution from the Department of Chemistry and the Materials Research Center, Northwestern University, Evanston, Illinois 60208-3113

Received September 20, 1993*

Abstract: This contribution describes the use of the computationally efficient, chemically-oriented INDO-SOS electronic structure model (ZINDO) to elucidate the electronic origins of the second-order nonlinear optical (NLO) response in molecules with extended π -architectures weakly coupled to transition-metal fragments. ZINDO-derived quadratic hyperpolarizabilities are found to be in excellent agreement with experiment for a variety of group 6 pyridine pentacarbonyl complexes in which coordination to the low-valent metal fragments *enhances* the NLO response of the free ligands. The metal–pyridine chromophores are found to obey the classical two-level model. However, the β -dictating MLCT transitions possess significantly larger $\Delta\mu_{ge}$ values and markedly lower oscillator strengths relative to the traditional organic chromophore π -donor–acceptor architectures by virtue of weak coupling between the metal and the ligand π -network. The computed quadratic hyperpolarizabilities of group 6 stilbazole pentacarbonyl derivatives are in good agreement with experiment. In contrast to conventional organic chromophores, an increase in π -conjugation length of the stilbazole ligands *does not* result in a dramatic increase in the second-order response or a decrease in the HOMO \rightarrow LUMO transition energy. The molecular orbital analysis indicates that the metal pentacarbonyl fragment acts as σ -acceptor, forcing the adjacent pyridine ring to become the molecular LUMO. As a consequence, the seemingly innocent pyridine ring becomes a primary charge acceptor in these structures, regardless of the derivatization or conjugation length. The synthesis and characterization of the donor-functionalized chromophore (4-(dimethylamino)-4'-stilbazole)W(CO)₅ is also reported. The large observed β_{vec} value supports the proposed NLO response model.

Introduction

An understanding of the electronic origin of molecular nonlinear optical (NLO) response is of fundamental scientific interest as well as a crucial component in the development of state-of-the-art NLO materials.^{1,2} Quantum chemical chromophore structure–NLO response analyses permit researchers to identify the electronic structure signatures characteristic of enhanced microscopic NLO response, and ultimately to design molecular structures with potentially optimal NLO susceptibilities. Once promising chromophoric structures are identified, they can be incorporated into a variety of macroscopic architectures, such as

self-assembled superlattices³ or poled polymer films,⁴ to yield molecule-based second-order photonic materials with superior optical, physical, and fabrication properties.^{1,2}

Organometallic structures are intriguing candidates for study as second-order NLO chromophores by virtue of their low-energy, yet sometimes intense, electronic charge-transfer excitations.⁵ Such *linear* optical characteristics are suggestive signatures of molecules exhibiting significant, second-order *nonlinear* optical response.⁶ In the late 1980s, *trans*-1-ferrocenyl-2-(*N*-methylpyridinium-4-yl)ethylene iodide⁷ (**1**) and *cis*-1-ferrocenyl-2-(4-nitrophenyl)ethylene⁸ (**2**) were found to possess rather large powder second harmonic generation (SHG) efficiencies (~ 220 and ~ 62 times that of urea, respectively), motivating many organometallic chemists to enter the field. As a result, a number of reports of macroscopic^{9–12} and microscopic^{13–15} responses for

* Abstract published in *Advance ACS Abstracts*, August 15, 1994.

(1) (a) Boyd, R. W. *Nonlinear Optics*; Academic Press: New York, 1992. (b) Prasad, N. P.; Williams, D. J. *Introduction to Nonlinear Optical Effects in Molecules and Polymers*; Wiley: New York, 1991. (c) Eaton, D. F. *Science* **1991**, *253*, 281–287. (d) Marder, S. R.; Beratan, D. N.; Cheng, L.-T. *Science* **1991**, *252*, 103–106. (e) Zyss, J. *J. Mol. Electron.* **1985**, *1*, 25–56. (f) Williams, D. J. *Angew. Chem., Int. Ed. Engl.* **1984**, *23*, 690–703. (g) Shen, Y. R. *The Principles of Nonlinear Optics*; Wiley: New York, 1984.

(2) (a) Williams, D. J., Ed. *Nonlinear Optical Properties of Organic Molecules V*. *SPIE Proc.* **1992**, *1775*. (b) Marder, S. R.; Sohn, J. E.; Stucky, G. D., Eds. *Materials for Nonlinear Optics: Chemical Perspectives*; ACS Symposium Series 455; American Chemical Society: Washington, DC, 1991. (c) Brédas, J. L.; Silbey, R. J., Eds. *Conjugated Polymers. The Novel Science and Technology of Highly Conducting and Nonlinear Optically Active Materials*; Kluwer: Dordrecht, Netherlands, 1991. (d) Khanarian, G., Ed. *Nonlinear Optical Properties of Organic Molecules III*. *SPIE Proc.* **1990**, *1337*. (e) Khanarian, G., Ed. *Nonlinear Optical Properties of Organic Molecules II*. *SPIE Proc.* **1990**, *1147*. (f) Heeger, A. J.; Orenstein, J.; Ulrich, D. R., Eds. *Nonlinear Optical Properties of Polymers*. *Mater. Res. Soc. Symp. Proc.* **1988**, *109*. (g) Hann, R. A.; Bloor, D., Eds. *Organic Materials for Nonlinear Optics*; Royal Society of Chemistry Monograph 69; Burlington House: London, 1988. (h) Chemla, D. S.; Zyss, J., Eds. *Nonlinear Optical Properties of Organic Molecules and Crystals*; Academic Press: New York, 1987; Vols. 1, 2. (i) Williams, D. J., Ed. *Nonlinear Optical Properties of Organic Molecules and Polymeric Materials*; ACS Symposium Series 233; American Chemical Society: Washington, DC, 1984. (j) Optical Nonlinearities in Chemistry. *Chem. Rev.* **1994**, *94*, Issue No. 1 (Introduction by Burland, D. M.).

(3) (a) Kakkar, A. K.; Yitzchaik, S.; Roscoe, S. B.; Kubota, F.; Allan, D. S.; Marks, T. J.; Lin, W. P.; Wong, G. K. *Langmuir* **1993**, *9*, 388–390. (b) Li, D. Q.; Ratner, M. A.; Marks, T. J.; Zhang, C. H.; Yang, J.; Wong, G. K. *J. Am. Chem. Soc.* **1990**, *112*, 7389–7390.

(4) (a) Hubbard, M. A.; Marks, T. J.; Lin, W. P.; Wong, G. K. *Chem. Mater.* **1992**, *4*, 965–968. (b) Lin, J. T.; Hubbard, M. A.; Marks, T. J.; Lin, W. P.; Wong, G. K. *Chem. Mater.* **1992**, *4*, 1148–1150.

(5) See, for example: (a) Lever, A. B. P. *Inorganic Electronic Spectroscopy*, 2nd ed.; Elsevier: Amsterdam, 1984; Chapter 5. (b) Geoffroy, G. L.; Wrighton, M. S. *Organometallic Photochemistry*; Academic Press: New York, 1979; Chapter 1.

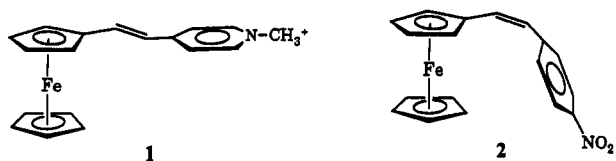
(6) (a) Oudar, J. L. *J. Chem. Phys.* **1977**, *67*, 446–457. (b) Oudar, J. L.; Chemla, D. S. *J. Chem. Phys.* **1977**, *66*, 2664–2668.

(7) Marder, S. R.; Perry, J. W.; Schaefer, W. P.; Tiemann, B. G.; Groves, P. C.; Perry, J. W. Reference 2e, pp 108–115.

(8) Green, M. L. H.; Marder, S. R.; Thompson, M. E.; Bandy, J. A.; Bloor, D.; Kolinsky, P. V.; Jones, R. J. *Nature* **1987**, *330*, 360–362.

(9) (a) Pollagi, T. P.; Stoner, T. C.; Dallinger, R. F.; Gilbert, T. M.; Hopkins, M. D. *J. Am. Chem. Soc.* **1991**, *113*, 703–704. (b) Wright, M. E.; Toplikar, E. G.; Kubin, R. F.; Seltzer, M. D. *Macromolecules* **1992**, *25*, 1838–1839. (c) Chiang, W.; Thompson, M. E.; Van Engen, D. *Spec. Publ.—R. Soc. Chem.* **1991**, *91* (Org. Mater. Non-linear Opt. 2), 210–216.

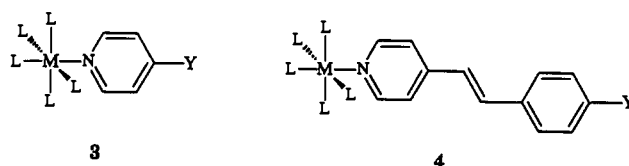
organotransition-metal¹⁶ systems have appeared in the recent literature. Architectures such as metal-containing polymers,⁹ classical coordination compounds,^{10,11,13,15} and metallocene structures¹²⁻¹⁴ have been the subject of these studies. Despite



these intense synthetic efforts, however, the measured NLO responses of the metal-containing chromophores prepared to date are almost invariably lower than those of typical π -organic donor-acceptor chromophores of comparable molecular dimensions.¹⁷ Moreover, the beginning of an electronic-structure-based understanding as to why the metal-organic molecules typically exhibit considerably smaller responses than their π -organic counterparts was not available until a recent ZINDO-SOS study on η^5 -ferrocenyl and η^6 -chromium arene chromophores.¹⁸ This study concluded that the electronic environments about the metal centers in the subject complexes are essentially pseudocen-

trosymmetric and, therefore, lack the extreme electronic asymmetry required for large second-order responses.

In this contribution, we employ the ZINDO-SOS formalism to analyze the NLO characteristics of molecular topologies containing an organometallic fragment coupled to a π -ligand in an η^1 fashion (L_5ML' , where L represents a common ancillary ligand and L' and extended π -organic system) as chromophores in NLO materials. These motifs offer attractive alternatives to the aforementioned η^5 -ferrocenyl complexes and the η^6 -chromium arene structures by virtue of topological similarity to conventional push-pull organic chromophores. The representative molecular classes discussed herein will include (pyridine) ML_5 molecules (3) and (stilbazole) ML_5 derivatives (4). Recently, a number of



nitrogen-bound organometallic chromophores have been investigated experimentally both in this laboratory and elsewhere^{13,15} and will serve as benchmarks for correlating theory and experiment. The chemically-oriented, computationally-efficient ZINDO-SOS scheme enables us to understand observed NLO responses, to advance a general prescription for optimizing the β tensor for a given class of chromophores, and to determine if particular molecular architectures are viable alternatives to classical donor-acceptor polyene chromophore structures. In this study, we show that while the molecular topologies of the transition metal chromophores are very reminiscent of high- β organic molecules, the mechanism of the NLO response is distinctly different. To calibrate our theoretical predictions, the model chromophore (4-(dimethylamino)-4'-stilbazole)WCO₅ was synthesized, characterized, and the NLO response evaluated.

Computational Methodology

A quantitative description of the molecular NLO response is derived from a power series expansion of the induced molecular dipole moment (polarization) upon interaction with light waves (oscillating external electric field E) (eq 1).¹ Here p_i is the

$$p_i = \sum_j \alpha_{ij} E_j + \sum_{j \geq k} \beta_{ijk} E_j E_k + \sum_{j \geq k \geq l} \gamma_{ijkl} E_j E_k E_l + \dots \quad (1)$$

molecular polarization induced in the i th Cartesian direction and is a function of the input laser frequency (ω), E_j is the j th Cartesian component of the applied electric field, α is the linear polarizability, β is the quadratic susceptibility, and γ is the cubic hyperpolarizability. The α coefficient represents the linear response of the electron cloud to an applied field; the higher order terms represent the nonlinear response. The β tensor is responsible for second harmonic generation (SHG) and will be the focus of the present work. Note that the chromophore-dependent α , β , and γ coefficients are extremely sensitive to the electronic environment and, therefore, exhibit a high degree of tailorability with molecular geometry.¹⁷

Several schemes for accurately calculating β tensors have appeared in the literature.^{18b,19} The preferred quantum me-

(18) (a) Kanis, D. R.; Ratner, M. A.; Marks, T. J. *J. Am. Chem. Soc.* **1992**, *114*, 10338-10357. (b) Kanis, D. R.; Ratner, M. A.; Marks, T. J. *Chem. Rev.* **1994**, *94*, 195-242.

(19) There are several definitional issues associated with comparing calculated microscopic responses to those obtained via experiment (see, for example: Willetts, A.; Rice, J. E.; Burland, D. M.; Shelton, D. P. *J. Chem. Phys.* **1992**, *97*, 7590-7599). The issues of concern in this contribution are the definition of molecular hyperpolarizability (Taylor series or perturbation series convention) and the definition of electric fields (real or complex). The theoretically-derived β values in this contribution and the reported EFISH-derived reference values for DANS both employ the "Ward" definition.

(10) (a) Coe, B. J.; Jones, C. J.; McCleverty, J. A.; Bloor, D.; Kolinsky, P. V.; Jones, R. J. *J. Chem. Soc., Chem. Commun.* **1989**, 1485-1487. (b) Coe, B. J.; Kurek, S. S.; Rowley, N. M.; Foulon, J. D.; Hamor, T. A.; Harman, M. E.; Hursthouse, M. B.; Jones, C. J.; McCleverty, J. A.; Bloor, D. *Chemtronics* **1991**, *5*, 23-28. (c) Zhang, N.; Jiang, M. H.; Yuan, D. R.; Xu, D.; Tao, X. T.; Shao, Z. S. *J. Cryst. Growth* **1990**, *102*, 581-584. (d) Tao, X.; Zhang, N.; Yuan, D.; Xu, D.; Yu, W.; Jiang, M. Reference 2e, pp 385-389. (e) Eaton, D. F.; Anderson, A. G.; Tam, W.; Wang, Y. *J. Am. Chem. Soc.* **1987**, *109*, 1886-1888. (f) Anderson, A. G.; Calabrese, J. C.; Tam, W.; Williams, I. D. *Chem. Phys. Lett.* **1987**, *134*, 392-396. (g) Tam, W.; Eaton, D. F.; Calabrese, J. C.; Williams, I. D.; Wang, Y.; Anderson, A. G. *Chem. Mater.* **1989**, *1*, 128-140. (h) Tam, W.; Calabrese, J. C. *Chem. Phys. Lett.* **1988**, *144*, 79-82. (i) Lamberth, C.; Murphy, D. M.; Mingos, D. M. P. *Spec. Publ.-R. Soc. Chem.* **1991**, *91* (Org. Mater. Non-linear Opt. 2), 183-189. (j) Copley, R. C. B.; Lamberth, C.; Machell, J.; Mingos, D. M. P.; Murphy, D. M.; Powell, H. J. *Mater. Chem.* **1991**, 583-589. (k) Lesley, G.; Yuan, Z.; Stringer, I.; Jobe, I. R.; Taylor, N. J.; Koch, L.; Scott, K.; Marder, T. B.; Williams, I. D.; Kurtz, S. K. *Spec. Publ.-R. Soc. Chem.* **1991**, *91* (Org. Mater. Non-linear Opt. 2), 197-203. (l) Sakaguchi, H.; Nagamura, T.; Matsuo, T. *Appl. Organomet. Chem.* **1991**, *5*, 257-260. (m) Thami, T.; Bassoul, P.; Petit, M. A.; Simon, J.; Fort, A.; Barzoukas, M.; Villaeys, A. *J. Am. Chem. Soc.* **1992**, *114*, 915-921. (n) Yuan, D.; Zhang, N.; Tao, X.; Xu, D.; Jiang, M.; Shao, Z. *Chin. Sci. Bull.* **1991**, *36*, 1401-1404. (o) Marcy, H. O.; Warren, L. F.; Webb, M. S.; Ebberts, C. A.; Velsko, S. P.; Kennedy, G. C.; Catella, G. C. *Appl. Opt.* **1992**, *31*, 5051-5060. (p) Chollet, P. A.; Kajzar, F.; Moigne, J. L. *SPIE-Int. Soc. Opt. Eng.* **1990**, *1273*, 87-95.

(11) (a) Frazier, C. C.; Harvey, M. A.; Cockerham, M. P.; Hand, H. M.; Chauchard, E. A.; Lee, C. H. *J. Phys. Chem.* **1986**, *90*, 5703-5706. (b) Calabrese, J. C.; Tam, W. *Chem. Phys. Lett.* **1987**, *133*, 244-245. (12) (a) Bunting, H. E.; Green, M. L. H.; Marder, S. R.; Thompson, M. E.; Bloor, D.; Kolinsky, P. V.; Jones, R. J. *Polyhedron* **1992**, *11*, 1489-1499. (b) Bandy, J. A.; Bunting, H. E.; Garcia, M. H.; Green, M. L. H.; Marder, S. R.; Thompson, M. E.; Bloor, D.; Kolinsky, P. V.; Jones, R. J.; Perry, J. W. *Polyhedron* **1992**, *11*, 1429-1435. (c) Marder, S. R.; Perry, J. W.; Tiemann, B. G.; Schaefer, W. P. *Organometallics* **1991**, *10*, 1896-1901. (d) Bandy, J. A.; Bunting, H. E.; Garcia, M. H.; Green, M. L. H.; Marder, S. R.; Thompson, M. E.; Bloor, D.; Kolinsky, P. V.; Jones, R. J. Reference 2g, pp 225-231. (e) Houlton, A.; Jasim, N.; Roberts, R. M. G.; Silver, J.; Cunningham, D.; McArdle, P.; Higgins, T. J. *Chem. Soc., Dalton Trans.* **1992**, 2235-2241. (f) Doisneau, G.; Balavoine, G.; Fillebeen-Khan, T.; Clinet, J. C.; Delaire, J.; Ledoux, I.; Loucif, R.; Puccetti, G. *J. Organomet. Chem.* **1991**, *421*, 299-304. (g) Richardson, T.; Roberts, G. G.; Polywka, M. E. C.; Davies, S. G. *Thin Solid Films* **1989**, *179*, 405-411. (h) Kimura, M.; Abel-Halim, H.; Robinson, D. W.; Cowan, D. O. *J. Organomet. Chem.* **1991**, *403*, 365-372. (i) Yamazaki, Y.; Hosono, K.; Matsuda, H.; Minami, N.; Asai, M.; Nakanishi, H. *Biotechnol. Bioeng.* **1991**, *38*, 1218-1222. (j) Qin, J.; Gong, X.; Wu, X.; Liao, J.; Dai, C.; Gu, J.; Ma, S.; Liu, D. *C-MRS Int. Symp. Proc.* **1991**, *1*, 409-412.

(13) Cheng, L.-T.; Tam, W.; Meredith, G. R.; Marder, S. R. *Mol. Cryst. Liq. Cryst.* **1990**, *189*, 137-153.

(14) Calabrese, J. C.; Cheng, L.-T.; Green, J. C.; Marder, S. R.; Tam, W. *J. Am. Chem. Soc.* **1991**, *113*, 7227-7232.

(15) (a) Cheng, L.-T.; Tam, W.; Eaton, D. F. *Organometallics* **1990**, *9*, 2856-2857. (b) Di Bella, S.; Fragalà, I.; Ledoux, I.; Diaz-García, M. A.; Lacroix, P. G.; Marks, T. J. *Chem. Mater.* **1994**, *6*, 881-883.

(16) (a) Nalwa, H. S. *Appl. Organomet. Chem.* **1991**, *5*, 349-377. (b) Long, N. J. *Angew. Chem., Int. Ed. Engl.*, in press.

(17) (a) Cheng, L.-T.; Tam, W.; Stevenson, S. H.; Meredith, G. R. *J. Phys. Chem.* **1991**, *95*, 10631-10643. (b) Cheng, L.-T.; Tam, W.; Marder, S. R.; Steigman, A. E.; Rikken, G.; Spangler, C. W. *J. Phys. Chem.* **1991**, *95*, 10643-10652.

chanical formalism would employ an ab initio electronic structure model, with a large basis set containing diffuse and polarization functions incorporating electron correlation, and explicitly including the optical field in the molecular Hamiltonian. To date, such computationally-intensive ab initio procedures could only be implemented for molecules of limited size.²⁰ The number of valence electrons in the chromophoric structures examined herein, as well as the current lack of suitable extended transition-metal basis sets, precludes us from employing any of these computationally-demanding treatments in the present study. Rather, computational procedures based upon an approximate Hamiltonian will be more appropriate for treating these elaborate structures. As an example, the MNDO (modified intermediate neglect of differential overlap) paradigm has been used in concert with a finite-field formalism, for example, to compute the nonlinear optical response.²¹ In this contribution, the hyperpolarizability will be computed using a sum over excited particle-hole states (SOS) approach. Since the NLO expansion coefficients in this formalism are functions of linear optical properties (such as excitation energies and dipole matrix elements), the necessary SOS electronic structure information can be conveniently obtained from a spectroscopically-based semiempirical electronic structure model. Indeed, previous SOS studies have employed either a modified all-valence CNDO/S²² (complete neglect of differential overlap), a π -electron PPP²³ (Parr-Pariser-Pople), or more recently, an all-valence INDO/S^{18,24-28} (intermediate neglect of differential overlap) model Hamiltonian to compute frequency doubling efficiencies. These computationally-efficient, chemically-oriented, quantum chemical methods have been successful

(20) (a) Sekino, H.; Bartlett, R. *Int. J. Quantum Chem.* **1992**, *43*, 119–134. (b) Sekino, H.; Bartlett, R. *J. Chem. Phys.* **1991**, *94*, 3665–3669. (c) Sekino, H.; Bartlett, R. *J. Chem. Phys.* **1986**, *85*, 976–989. (d) Jaszufski, M.; Jørgensen, P.; Jensen, H. J. A. *Chem. Phys. Lett.* **1992**, *191*, 293–298. (e) Aiga, F.; Sasagane, K.; Itoh, R. *Chem. Phys.* **1992**, *167*, 277–290. (f) Hammond, B. L.; Rice, J. E. *J. Chem. Phys.* **1992**, *97*, 1138–1143. (g) Rice, J. E.; Amos, R. D.; Colwell, S. M.; Handy, N. C.; Sanz, J. J. *Chem. Phys.* **1990**, *93*, 8828–8839. (h) Sim, F.; Chin, S.; Dupuis, M.; Rice, J. E. *J. Phys. Chem.* **1993**, *97*, 1158–1163. (i) Meyers, F.; Brédas, J. L.; Zyss, J. *J. Am. Chem. Soc.* **1992**, *114*, 2914–2921. (j) Tsunekawa, T.; Yamaguchi, K. *Chem. Phys. Lett.* **1992**, *190*, 533–538. (k) Karna, S. P.; Prasad, P. N.; Dupuis, M. *J. Chem. Phys.* **1991**, *94*, 1171–1181. (l) Karna, S. P.; Dupuis, M. *J. Comput. Chem.* **1991**, *12*, 487–504. (m) Daniel, C.; Dupuis, M. *Chem. Phys. Lett.* **1990**, *171*, 209–216. (n) Keshar, V.; Karna, S. P.; Prasad, P. N. *J. Phys. Chem.* **1993**, *97*, 3525–3529. (o) Sekino, H.; Bartlett, R. *J. Chem. Phys.* **1993**, *98*, 3022–3027. (p) Shelton, D. P.; Rice, J. E. *Chem. Rev.* **1994**, *94*, 3–29.

(21) (a) Matsuzawa, N.; Dixon, D. A. *J. Phys. Chem.* **1992**, *96*, 6232–6241. (b) Barzoukas, M.; Fort, A.; Klein, G.; Serbutoviez, C.; Oswald, L.; Nicoud, J. F. *Chem. Phys.* **1992**, *164*, 395–406. (c) Subramaniam, G.; Polashenski, S.; Kennedy, K. *Ferroelectrics* **1991**, *122*, 229–238. (d) Kurtz, H. A.; Stewart, J. J. P.; Dieter, K. M. *J. Comput. Chem.* **1990**, *11*, 82–87. (e) Waite, J.; Papadopoulos, M. G. *J. Phys. Chem.* **1990**, *94*, 1755–1758.

(22) (a) Morley, J. O.; Pugh, D. J. *Chem. Soc., Faraday Trans.* **1991**, *87*, 3021–3025. (b) Docherty, V. J.; Pugh, D.; Morley, J. O. *J. Chem. Soc., Faraday Trans. 2* **1985**, *81*, 1179–1192. (c) Lalama, S. L.; Garito, A. F. *Phys. Rev.* **1979**, *20*, 1179–1194. (d) Morrell, J. A.; Albrecht, A. C. *Chem. Phys. Lett.* **1979**, *64*, 46–50. (e) Munn, R. W. *Int. J. Quantum Chem.* **1992**, *43*, 159–169. (f) Maslianitsin, I. A.; Shigorin, V. D.; Shipulo, G. P. *Chem. Phys. Lett.* **1992**, *194*, 355–358. (g) Sen, R.; Majumdar, D.; Bhattacharyya, S. P.; Bhattacharyya, S. N. *Chem. Phys. Lett.* **1991**, *181*, 288–292.

(23) (a) Li, D.; Ratner, M. A.; Marks, T. J. *J. Phys. Chem.* **1992**, *96*, 4325–4336. (b) Li, D.; Marks, T. J.; Ratner, M. A. *J. Am. Chem. Soc.* **1988**, *110*, 1707–1715. (c) Soos, Z. G.; Ramasesha, S. *J. Chem. Phys.* **1989**, *90*, 1067–1076. (d) Albert, I. D. L.; Das, P. K.; Ramasesha, S. *Chem. Phys. Lett.* **1991**, *176*, 217–224. (e) de Melo, C. P.; Silbey, R. J. *Chem. Phys.* **1988**, *88*, 2567–2571. (f) Dirk, C. W.; Twieg, R. J.; Wagniere, G. J. *Am. Chem. Soc.* **1986**, *108*, 5387–5395.

(24) (a) Brédas, J. L.; Meyers, F.; Pierce, B. M.; Zyss, J. *J. Am. Chem. Soc.* **1992**, *114*, 4928–4929. (b) Gao, X. L.; Feng, J. K.; Sun, C. C. *Int. J. Quantum Chem.* **1992**, *42*, 1747–1758. (c) Ulman, A.; Willand, C. S.; Kohler, W.; Robello, D. R.; Williams, D. J.; Handley, L. *J. Am. Chem. Soc.* **1990**, *112*, 7083–7090. (d) Ulman, A. *J. Phys. Chem.* **1988**, *92*, 2385–2390. (e) Parkinson, W. A.; Zerner, M. C. *J. Chem. Phys.* **1989**, *90*, 5606–5611.

(25) Kanis, D. R.; Marks, T. J.; Ratner, M. A. *Int. J. Quantum Chem.* **1992**, *43*, 61–82.

(26) Kanis, D. R.; Ratner, M. A.; Marks, T. J.; Zerner, M. C. *Chem. Mater.* **1991**, *3*, 19–22.

(27) Kanis, D. R.; Ratner, M. A.; Marks, T. J. *J. Am. Chem. Soc.* **1990**, *112*, 8203–8204.

(28) Kanis, D. R.; Marks, T. J.; Ratner, M. A. *Nonlinear Optics* **1994**, *6*, 317–335.

at both describing and understanding observed NLO responses for complex chromophoric structures, such as those examined in this contribution. Specifically, we employ here the transition-metal INDO/S formalism (ZINDO)²⁹ to describe the second-order NLO response of transition-metal-containing chromophores.

The ZINDO-SOS quantum chemical approach^{18,25-28} incorporates a well-defined model Hamiltonian and a perturbation-based formalism to calculate quadratic hyperpolarizabilities (β) for potential chromophoric structures. The algorithm initially computes wave functions and relative energy differences for the ground state and excited states of a given molecular geometry using the semiempirical ZINDO model. The relevant electronic structure information serves as input into a SOS quantum mechanical prescription³⁰ where the ground state is taken as the Hartree-Fock single determinant, and the electronic states created by the perturbing laser field are treated as an infinite sum over unperturbed particle-hole states. The individual tensorial components of the quadratic hyperpolarizability are given by eq 2,³⁰

$$\beta_{ijk} + \beta_{ikj} = -\frac{e^3}{4\hbar^2} \left[\sum_{n' \neq g} \sum_{\substack{n'' \neq g \\ n'' \neq n'}} \left\{ (r_{gn'}^j r_{n'n''}^i r_{n''gn}^k + r_{gn'}^k r_{n'n''}^i r_{n''gn}^j) \times \left(\frac{1}{(\omega_{n'g} - \omega)(\omega_{ng} + \omega)} + \frac{1}{(\omega_{n'g} + \omega)(\omega_{ng} - \omega)} \right) + (r_{gn'}^i r_{n'n''}^j r_{n''gn}^k + r_{gn'}^k r_{n'n''}^j r_{n''gn}^i) \times \left(\frac{1}{(\omega_{n'g} + 2\omega)(\omega_{ng} + \omega)} + \frac{1}{(\omega_{n'g} - 2\omega)(\omega_{ng} - \omega)} \right) + (r_{gn'}^j r_{n'n''}^k r_{n''gn}^i + r_{gn'}^i r_{n'n''}^k r_{n''gn}^j) \times \left(\frac{1}{(\omega_{n'g} - \omega)(\omega_{ng} - 2\omega)} + \frac{1}{(\omega_{n'g} + \omega)(\omega_{ng} + 2\omega)} \right) \right\} + 4 \sum_{n \neq g} \left\{ [r_{gn}^j r_{gn}^k \Delta r_n^i (\omega_{ng}^2 - 4\omega^2) + r_{gn}^i (r_{gn}^j \Delta r_n^k + r_{gn}^k \Delta r_n^j) (\omega_{ng}^2 + 2\omega^2)] \times \frac{1}{(\omega_{ng}^2 - \omega^2)(\omega_{ng}^2 - 4\omega^2)} \right\} \right] \quad (2)$$

where ω is the incident frequency of the optical field, $r_{n'n}^i = \langle \psi_n | r^i | \psi_n \rangle$ is the matrix element of the displacement operator $r^{(i)}$ along the i th molecular axis between electronic states ψ_n and ψ_n , $\Delta r_n^i = r_{nn}^i - r_{gg}^i$ is the dipole moment difference between excited state and ground state (denoted by n and g , respectively), and $\hbar\omega_{ng}$ is the eigenvalue of the excited state (ψ_n) relative to the ground state. The transition moment matrix elements are straightforwardly computed in dipole length form using LCAO-MO coefficients and the Pariser approximation³¹ for matrix elements over atomic orbitals (κ, λ ; eq 3), where $R_{\kappa\lambda}^i$ are nuclear coordinates.

$$r_{\kappa\lambda}^i = \delta_{\kappa\lambda} R_{\kappa\lambda}^i \quad (3)$$

In this approach, as in other semiempirical treatments that compute linear and nonlinear optical properties, the monoexcited

(29) (a) Anderson, W. P.; Cundari, T. R.; Drago, R. S.; Zerner, M. C. *Inorg. Chem.* **1990**, *29*, 1–3. (b) Kotzian, M.; Rösch, N.; Schröder, H.; Zerner, M. C. *J. Am. Chem. Soc.* **1989**, *111*, 7687–7696. (c) Anderson, W. P.; Edwards, W. D.; Zerner, M. C. *Inorg. Chem.* **1986**, *25*, 2728–2732. (d) Zerner, M. C.; Loew, G. H.; Kirchner, R. F.; Mueller-Westerhoff, U. T. *J. Am. Chem. Soc.* **1980**, *102*, 589–599. (e) Bacon, A. D.; Zerner, M. C. *Theor. Chim. Acta (Berlin)* **1979**, *53*, 21–54. (f) Ridley, J.; Zerner, M. C. *Theor. Chim. Acta (Berlin)* **1973**, *32*, 111–134.

(30) Ward, J. F. *Rev. Mod. Phys.* **1971**, *37*, 1–18.

(31) Pariser, R.; Parr, R. G. *J. Chem. Phys.* **1953**, *21*, 466–471.

configuration interaction (MECI) approximation³² is employed to describe the excited states. In principle, all possible monoexcited states should be included in the summation over ψ_n and ψ_n' in eq 2; however, it has been shown that the computed second-order response converges without including all possible excited states of the valence basis.^{18,22b,24c,25} For the present ZINDO-SOS NLO computations, the SOS summation was restricted (eq 2) to the 100 excited configurations of lowest energy. This has proven to be a valid assumption in computing β_{vec} for archetypical donor-acceptor π -electron organic chromophores,²⁵ as well as for representative ferrocenyl and chromium-arene transition-metal chromophores.^{18a}

The ZINDO-SOS method computes all 27 of the components of β ; however, only the vector component along the dipole moment direction, β_{vec} (eq 4), is sampled experimentally in electric field induced second harmonic generation (EFISH) experiments.³³ Thus,

$$\beta_{vec}(-2\omega; \omega, \omega) = \sum_{i=1}^3 \frac{\mu_i \beta_i}{|\mu|} \quad (4)$$

where

$$\beta_i = \beta_{iii} + \frac{1}{3} \sum_{j \neq i} (\beta_{ijj} + \beta_{jij} + \beta_{jji}) \quad (5)$$

μ is the ground state molecular dipole moment, and i and j run over the molecular directions x , y , and z .

The literature β_{vec} values (experimental) quoted in this contribution are taken from an internally consistent set of EFISH data.^{13,15,17} In using EFISH results from a single laboratory, we minimize deviations due to experimental conditions such as differing incident frequencies, solvent polarities, local field models, and data reduction schemes. All experimental and calculated nonresonant responses in this contribution (with the exception of EFISH data on the model chromophore 4-(dimethylamino)-4'-stilbazole)W(CO)₅ are measured at a fundamental photon energy of 0.65 eV (1907 nm). This particular photon energy is sufficiently removed from optical transitions that dispersive enhancement of the response should be minimized. All EFISH, optical spectroscopic, and dipole moment data quoted in this work were measured in relatively apolar solvents^{13,15,17} (dioxane and chloroform), diminishing the effects of solvent-chromophore interactions.

The INDO/S (ZINDO) semiempirical formalism was implemented as described by Zerner and co-workers²⁹ without any parameter manipulation or basis function modifications. The semiempirical procedure was not reparametrized specifically for NLO response computations. The existing ZINDO scheme provides an accurate, chemically-oriented description of *linear* optical properties for a wide range of transition-metal-containing structures without requiring extensive computational resources^{29b-d} and should therefore be the ideal electronic structural platform for NLO response calculations of transition-metal systems. To illustrate the efficiency of the algorithm, we note that none of the NLO computations reported herein required more than 20 min of CPU time on a Stellar 2000 minisupercomputer.

The geometrical coordinates chosen for the present calculations were based on published crystallographic data. We have demonstrated that idealized nuclear coordinates are legitimate alternatives to optimized structures for input in NLO calculations,²⁵ and all molecular structures in this work were idealized in accord with the prescription reported.²⁵ Bond distances and angles in organic fragments were those given previously,^{18,25} where the bridging polyene structures employed bond-alternating

distance sequences of 1.44 Å–1.36 Å–1.44 Å. For the tungsten-pyridine complexes, the W atom was replaced with a Cr atom due to the present computational limitations of the ZINDO procedure. It is anticipated that this pragmatic Cr for W substitution will not greatly affect the calculated NLO properties since the *linear* optical properties (λ_{max} , f) in the Cr, Mo, W series of group 6 pyridine pentacarbonyl structures are nearly identical.^{5a,34} In accordance with the crystal structure of the parent (pyridine)Cr(CO)₅,³⁵ the pyridine ring was chosen to be planar, and the cis Cr–CO bonds were chosen to form 45° dihedral angles (staggered) with respect to the NC₅H₅ plane. The Cr–N bond distance was set at 2.165 Å, the cis Cr–CO distance at 1.905 Å (C–O distance at 1.141 Å), and the *trans* Cr–CO distance at 1.846 Å (C–O at 1.152 Å) for all chromophores in this class, in accordance with the crystal structure data.³⁵

Experimental Section

Materials and Methods. All synthetic operations were carried out with rigorous exclusion of oxygen using standard Schlenk techniques. Solvents were predried and distilled under prepurified nitrogen from appropriate drying agents. W(CO)₆ was obtained from Aldrich and used without further purification. ¹H NMR spectra were recorded on a Varian XL-400 spectrometer, optical spectra on a Perkin-Elmer 330 spectrometer, and infrared spectra on a Perkin-Elmer 283 instrument (calibrated with polystyrene). Optical spectroscopic oscillator strengths were calculated using the relationship $f = 4.315 \times 10^{-9} f_{\nu} dv$.⁵ Elemental analyses were performed by G. D. Searle, Inc.

Synthesis of (4-(Dimethylamino)-4'-stilbazole)tungsten Pentacarbonyl (6). Under a slow purge of N₂, W(CO)₆ (352 mg, 1.00 mmol) was photolyzed for 2 h in 150 mL of THF using a Pyrex-filtered high-pressure Hg lamp. The resulting (THF)W(CO)₅ solution was then transferred by cannula to a stirring solution of 224 mg (1.00 mmol) of 4-(dimethylamino)-4'-stilbazole (5)³⁶ in 50 mL of THF. The resulting red solution was stirred for 1 h and then evaporated to dryness in vacuo. The crude product was then purified by chromatography on silica (Merck, silica gel 60), eluting with 1:2 pentane CH₂Cl₂. Yield: 137 mg (25%) of red, polycrystalline material.

Anal. Calcd for C₂₀H₁₆N₂O₅W: C, 43.84; H, 2.92; N, 5.11. Found: C, 43.68; H, 2.90; N, 5.01. IR (cyclohexane): ν (CO) = 2069 (w), 1981 (w), 1930 (vs), 1914 (s); (KBr pellet) ν (CO) = 2069 (w), 1970 (m), 1947 (m), 1898 (vs), 1880 (s). ¹H NMR (CDCl₃): δ 8.509 (2H, d, J = 6.4 Hz), 7.436 (2H, d, J = 8.8 Hz), 7.316 (2H, d, J = 6.4 Hz), 7.243 (1H, d, J = 16.0 Hz), 6.799 (1H, d, J = 16.0 Hz), 6.712 (2H, d, J = 8.8 Hz), 3.011 (6H, s).

EFISH Measurements. The solution phase second-order response of complex 6 ($\mu \cdot \beta_{vec}$) was measured in dioxane solution using the dc field induced second harmonic generation (EFISH) instrumentation described previously.³⁷ The EFISH cell was enclosed in an anaerobic, N₂-purged metal box sealed with Viton O-rings and having two glass windows for the laser beam (1064 nm Q-switched YAG laser³⁷). The cell was filled (0.0020 M solutions) in a glovebox. The well-characterized organic chromophore 4-(dimethylamino)-4'-nitrostilbene (7; DANS) was employed as a standard (calibrant). All measurements were made in triplicate. Measurements on each sample as a function of time showed no evidence for sample decomposition over the course of several hours.

Data analysis was carried out as described previously.³⁷ This makes the reasonable assumption that electronic third-order (γ^e) and hyper-Raman contributions (γ^v) to the EFISH response are small relative to $\mu \cdot \beta_{vec}/5kT$.

Results and Discussion

Synthesis and NLO Response of the Model Chromophore (4-(Dimethylamino)-4'-stilbazole)tungsten Pentacarbonyl (6). The model tungsten pentacarbonyl chromophore, having a stilbazole ligand with a strong *electron-donating substituent*, was synthesized using conventional photochemical methodology (eqs 6 and 7).^{13,15}

(34) Reference 5b, Chapter 3, pp 45–58.

(35) Ries, W.; Bernal, I.; Quast, M.; Albright, T. A. *Inorg. Chim. Acta* 1984, 83, 5–15.

(36) Kuo, K. T. *J. Chin. Chem. Soc.* 1978, 25, 131–139.

(37) Saha, S. K.; Wong, G. K. *Appl. Phys. Lett.* 1979, 34, 423–425.

(32) Linderberg, J.; Öhrn, Y. *J. Chem. Phys.* 1967, 49, 716–727.

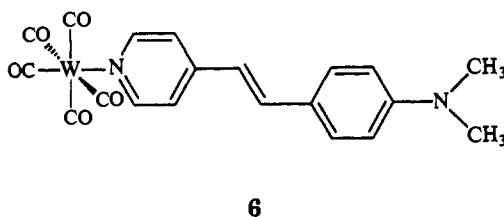
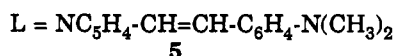
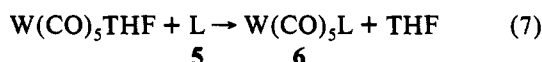
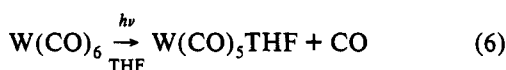
(33) Levine, B. F.; Bethea, C. G. *Appl. Phys. Lett.* 1974, 24, 445–447.

Table 1. EFISH and ZINDO-Derived Quadratic Hyperpolarizabilities for 4-(Dimethylamino)-4'-stilbazole (**5**) and (4-(Dimethylamino)-4'-stilbazole)W(CO)₅ (**6**) at 1.06 μm (ħω = 1.17 eV) Using 4-(Dimethylamino)-4'-nitrostilbene (**7**) as an Experimental Standard^{a,b}

	μ^{calc}	$\beta_{\text{vec}}^{\text{calc}}$	$(\mu \cdot \beta_{\text{vec}})^{\text{calc}}$	$(\mu \cdot \beta_{\text{vec}})^{\text{expt}}$	$\beta_{\text{vec}}^{\text{expt}}$
5	5.79	33.3	193	163 ^c	28.2 ^d
6	14.9	65.5	976	910 ^c	61.0 ^d
7	9.90	120	1190		
7		54.8 ^e			73 ^e

^a All NLO data are in units of 10⁻³⁰ cm⁵ esu⁻¹; all dipolar data are in debyes. ^b Note that M = Cr for all computed responses and M = W for experimental EFISH values. ^c Experimental EFISH data at 1.06 μm vs a **7** standard. Since μ·β_{vec} is only available at 1.91 μm (ħω = 0.65 eV) from ref 17, the ZINDO-computed value of 1190 × 10⁻³⁰ D·cm⁵ esu⁻¹ is used for **7**. ^d β_{vec} calculated by dividing the measured μ·β_{vec} by the ZINDO-derived μ value. ^e At 1.91 μm. Experimental datum from ref 17.

Characterization was by standard analytical and spectroscopic techniques.

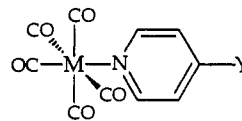


The experimentally-determined second-order susceptibilities of 4-(dimethylamino)-4'-stilbazole (**5**) and (4-(dimethylamino)-4'-stilbazole)W(CO)₅ (**6**), measured versus the DANS standard (**7**),¹⁷ are tabulated in Table 1 as are the ZINDO-derived responses. Note that the experimental results indicate that β_{vec} is enhanced when the organic ligand (β_{vec}^{expt} = 28.2 × 10⁻³⁰ cm⁵ esu⁻¹) is coordinated to a W(CO)₅ fragment (β_{vec}^{expt} for complex = 61.0 × 10⁻³⁰ cm⁵ esu⁻¹) at 1.06 μm. Interestingly, the experimental μ·β_{vec} response is approximately 5 times larger for the metal-coordinated chromophore relative to the isolated ligand (910 × 10⁻³⁰ D·cm⁵ esu⁻¹ versus 163 × 10⁻³⁰ D·cm⁵ esu⁻¹); however, the ZINDO computations suggest that approximately half the observed enhancement in μ·β_{vec} is actually due to the larger dipole moment of the metal complex versus the organic fragment, with the remainder due to an enhancement in the second-order tensor. The theoretical results listed in Table 1 are in excellent agreement with experiment, suggesting that, for this particular class of chromophores, the second-order response is indeed increased with the coordination to a metal fragment, in stark contrast to most metal-based chromophores reported in the literature to date. The remainder of the discussion will focus on understanding the electronic origin of the unusual second-order responses observed for group 6 pentacarbonylpyridine and then stilbazole complexes.

(Pyridine)M(CO)₅ Derivatives. Nonlinear Optical Responses.

A recent experimental study examined the NLO susceptibilities of various (pyridine)W(CO)₅ chromophores.^{13,15} The EFISH values and the present ZINDO-derived second-order responses for eight chromophores (**8–15**) of this type are given in Table 2. Note that the computed susceptibilities for M = Cr chromophores

Table 2. Comparison of Experimental and ZINDO-Derived Molecular Hyperpolarizabilities^{a,b} (β_{vec}), Two-Level Contributions to the Response (β_{vec,2}), and Three-Level Contributions (β_{vec,3}) to the Response at 1.91 μm (ħω = 0.65 eV) for a Series of Group 6 Pyridine Derivatives^b (For Purposes of Comparison, Data for *p*-Nitroaniline (**16**) and 4-Amino-4'-nitrostilbene (**17**) are Provided)



	Y	$\beta_{\text{vec}}^{\text{expt } c}$	$\beta_{\text{vec}}^{\text{calc}}$	$\beta_{\text{vec},2}^{\text{calc}}$	$\beta_{\text{vec},3}^{\text{calc}}$
8	NO ₂		-31.8	-50.8	19.0
9	COH	-12	-15.5	-29.2	13.7
10	COCH ₃	-9.3	-13.3	-25.1	11.8
11	C ₆ H ₅	-4.5	-4.49	-9.35	4.86
12	H	-4.4	-5.91	-10.4	4.51
13	C ₄ H ₉	-3.4	-3.98	-12.7	8.74
14	NH ₂	-2.1	-1.32	-3.24	1.92
15	N(CH ₃) ₂		0.55	0.19	0.36
16		9.2	10.7	17.2	-6.56
17		40	46.4	106	-59.1

^a All NLO data are in units of 10⁻³⁰ cm⁵ esu⁻¹. ^b Note that M = Cr for all computed responses and M = W for all EFISH values. ^c NLO data for transition-metal chromophores (**9–14**) are from refs 13 and 15; organic chromophore data are from ref 17.

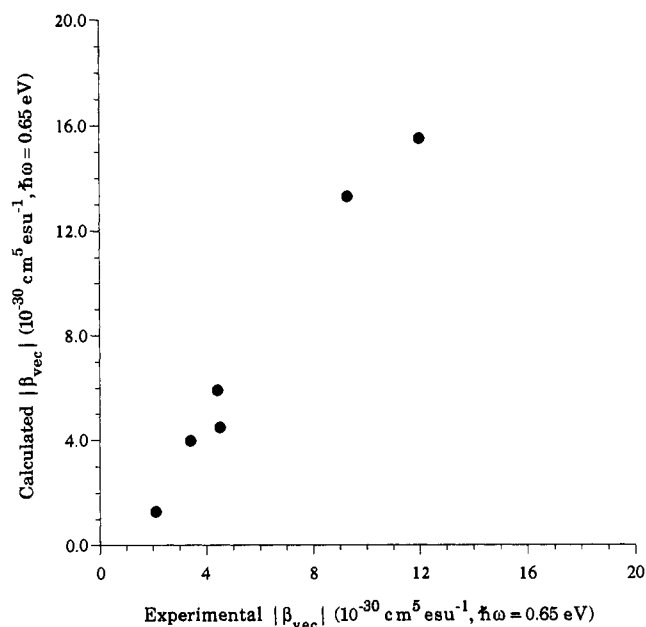
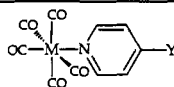
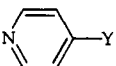


Figure 1. Plot of (pyridine)M(CO)₅ chromophore β_{vec} values computed by the ZINDO-SOS procedure versus experimental data from refs 13 and 15.

are in excellent agreement with the experimental responses for M = W molecules, as graphically illustrated in Figure 1. For example, the computed response for (4-benzylpyridine)Cr(CO)₅ (**11**, -4.49 × 10⁻³⁰ cm⁵ esu⁻¹) compares favorably with the EFISH value (-4.5 × 10⁻³⁰ cm⁵ esu⁻¹) for (4-benzylpyridine)W(CO)₅. Furthermore, the ZINDO-SOS algorithm also correctly predicts the negative β value observed experimentally. There is a systematic trend in both calculated and measured responses for these chromophores; namely, β_{vec} increases with the electron-accepting strength (in the Hammett sense) of the pyridine substituent. For example, β_{vec}^{calc} for (4-nitropyridine)Cr(CO)₅ > (4-formylpyridine)Cr(CO)₅ > (pyridine)Cr(CO)₅ > (4-aminopyridine)Cr(CO)₅.

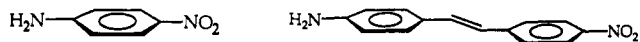
For comparative purposes, hyperpolarizability data for two prototypical organic chromophores, *p*-nitroaniline (**16**) and 4-amino-4'-nitrostilbene (**17**), are included in Table 2. These data reveal that the magnitudes of the second-order responses of the (pyridine)Cr(CO)₅ chromophores more closely resemble (in

Table 3. Comparison of ZINDO-Derived Molecular Hyperpolarizabilities^a (β_{vec}) for Pentacarbonyl(pyridine)chromium(0) Complexes and the Free Pyridine Ligands at 1.91 μm ($\hbar\omega = 0.65$ eV)

Y		
NO ₂	-31.8	1.69
COH	-15.5	-0.10
H	-5.91	-0.14
NH ₂	-1.32	1.57
N(CH ₃) ₂	0.55	2.60

^a All NLO data are in units of 10^{-30} cm⁵ esu⁻¹.

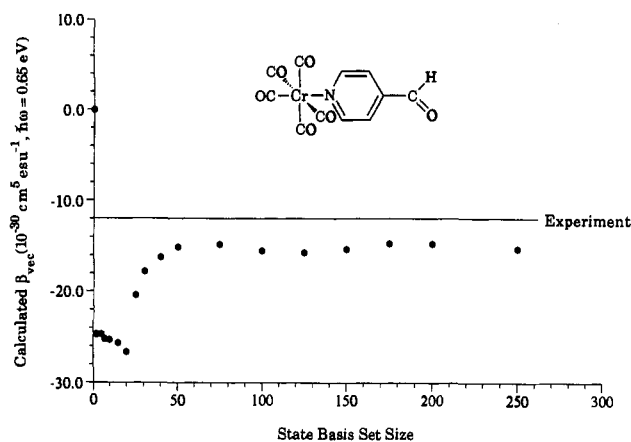
magnitude) push-pull phenylene structures than extended π systems, such as donor-acceptor stilbene architectures.



16

The qualitative mechanism that has been advanced^{13,15} to explain the EFISH data for the present class of chromophores assumes that one low-lying MLCT (metal-to-ligand charge-transfer) transition is responsible for the quadratic response within the SOS formalism. Such MLCT transitions have been observed and characterized in (pyridine)pentacarbonyltungsten(0) complexes.³⁸ With low-lying pyridine π^* orbitals readily available to the low-valent metal center, it is not surprising that these molecules possess $d_{\pi} \rightarrow \pi^*$ transitions. The observed negative second-order response is in accord with this hypothesis in that the ground state dipole moment will be strongly influenced by the σ -donation of nitrogen electrons into an empty metal orbital, which is antiparallel to the charge-transfer direction in the β -determining MLCT. These are precisely the conditions that would lead to a negative response within the framework of the two-level model.^{18b} Moreover, the large *negative solvatochromic behavior* associated with the MLCT band in such pyridine complexes³⁸ provides additional evidence that the dipole moment of the MLCT state is significantly smaller than the ground state dipole moment. It is interesting to compare the computed responses for the (4-Y-pyridine)M(CO)₅ complexes with those of the corresponding free 4-Y-pyridine ligands (Table 3). For Y = acceptor, the coordination of the metallic moiety greatly enhances the response, while for Y = donor, the hyperpolarizability is not greatly affected by the inclusion of the metal fragment. For example, the calculated quadratic hyperpolarizability for the formyl metal-coordinated chromophore (9, -15.5×10^{-30} cm⁵ esu⁻¹) is much greater than that for the free ligand (-0.10×10^{-30} cm⁵ esu⁻¹), yet the response for the metal-coordinated 4-aminopyridine chromophore (14) is essentially equal in magnitude to that for the isolated organic ligand (-1.32×10^{-30} cm⁵ esu⁻¹ versus 1.57×10^{-30} cm⁵ esu⁻¹). In accord with our findings for the model chromophore 4-(dimethylamino)-4'-stilbazole)W(CO)₅ (6, *vide supra*), the inclusion of a transition-metal substituent can tremendously enhance the second-order responsivity in these particular structures. This is in stark contrast to our previous findings with ferrocenyl and chromium arene chromophores.¹⁸

Deducing a Chemically-Oriented Explanation for β from the Computed Responses. The Assumptions. One of the principal objectives in performing computational studies on potential chromophoric candidates is to describe the computed responses in a chemically-oriented fashion. Since the ZINDO-SOS responses are in good agreement with those observed via EFISH measurements (Table 2), the algorithm can be used to pinpoint the origin of the NLO response in these chromophores and to

(38) Wrighton, M. S.; Abrahamson, H. B.; Morse, D. L. *J. Am. Chem. Soc.* 1976, 98, 4105-4109.**Figure 2.** Plot of ZINDO-derived β_{vec} values as a function of the number of state basis functions included in both configuration interaction and sum-over-states expansion for (4-formylpyridine)Cr(CO)₅.

validate the proposed electronic mechanism of the NLO response. In this section we shall briefly sketch the process by which such response “mechanisms” are extracted from ZINDO-SOS calculations and comment on the specific assumptions required to obtain such explanations.^{18,28} These concepts will then be applied to the metal-pyridine complexes.

Of the many hundreds of NLO chromophores that have been investigated in this laboratory via the ZINDO-SOS formalism (organic and organometallic), only a handful *do not* emulate the state basis set dependence shown pictorially in Figure 2 for (4-formylpyridine)Cr(CO)₅.³⁹ Note that the second-order response reaches a converged value (-15.5×10^{-30} cm⁵ esu⁻¹; in good agreement with the experimental response for the analogous tungsten chromophore of -12×10^{-30} cm⁵ esu⁻¹)¹⁵ with far less than 100 states included in the SOS summation, thus justifying the previously discussed truncated sum over excited states. Typically in plots of this sort, β_{vec} reaches a distinctive maximum early in the basis set summation, followed by a steep decline to approximately half the maximum value at convergence. A global description of the origin of these salient features can be grasped by partitioning the perturbative prescription for β into two components, $\beta_{\text{vec},2}$ and $\beta_{\text{vec},3}$, and then examining the contribution of each component to β_{vec} .

The sum-over-states expression (eq 2) can be decomposed into two general types of contributions, $\beta_{ijk,2}$ (eq 8) and $\beta_{ijk,3}$ (eq 9). Note that the $\beta_{ijk,2}$ expression (eq 8) contains only two states, a ground state (g) and one excited state (n), and the terms are therefore designated the “two-state” or more commonly the “two-level” terms. Likewise, the $\beta_{ijk,3}$ mathematical description contains a ground state (g) and *two* different excited states (n and n’), and the terms are referred to as “three-level” contributions. The prescriptions for converting the 27 individual tensorial elements into components along the ground state dipole moment direction ($\beta_{\text{vec},2}$ and $\beta_{\text{vec},3}$) are given by eqs 4 and 5. Ultimately, eq 10 is obtained, and we can then discuss the two-level and three-level components of the second-order response.

$$\beta_{ijk,2} = -\frac{e^3}{2\hbar^2} \sum_{n \neq g} \left\{ [r_{gn}^j r_{gn}^k \Delta r_n^i (\omega_{ng}^2 - 4\omega^2) + r_{gn}^i (r_{gn}^k \Delta r_n^j + r_{gn}^j \Delta r_n^k) (\omega_{ng}^2 + 2\omega^2)] \times \frac{1}{(\omega_{ng}^2 - \omega^2)(\omega_{ng}^2 - 4\omega^2)} \right\} \quad (8)$$

(39) It should be noted that the salient features of Figure 2 mimic those of previously published plots with one small difference. Since the calculated quadratic hyperpolarizability for the (pyridine)Cr(CO)₅ derivative is negative, the basis set convergence plot is a mirror image of those calculated for the more common positive- β chromophores. The implications of a sign difference in the intrinsic NLO response will become apparent.

$$\beta_{ijk,3} = -\frac{e^3}{8\hbar^2} \sum_{n \neq g} \sum_{n' \neq n} \left\{ \left(\frac{1}{(\omega_{n'g} - \omega)(\omega_{ng} + \omega)} + \frac{1}{(\omega_{n'g} + \omega)(\omega_{ng} - \omega)} \right) + \left(\frac{1}{(\omega_{n'g} - 2\omega)(\omega_{ng} - \omega)} + \frac{1}{(\omega_{n'g} + 2\omega)(\omega_{ng} + \omega)} \right) + \left(\frac{1}{(\omega_{n'g} - \omega)(\omega_{ng} - 2\omega)} + \frac{1}{(\omega_{n'g} + \omega)(\omega_{ng} + 2\omega)} \right) \right\} \times \left(r_{gn}^j r_{n'n}^i r_{gn}^k + r_{gn}^k r_{n'n}^i r_{gn}^j + r_{gn}^i r_{n'n}^k r_{gn}^j + r_{gn}^k r_{n'n}^j r_{gn}^i + r_{gn}^j r_{n'n}^k r_{gn}^i + r_{gn}^i r_{n'n}^j r_{gn}^k \right) \quad (9)$$

$$\beta_{\text{vec}} = \beta_{\text{vec},2} + \beta_{\text{vec},3} \quad (10)$$

As discussed in a recent contribution,¹⁸ not only are the shapes of basis set plots (e.g., Figure 2) essentially invariant for a wide range of chromophore types, but so are the relative contributions of $\beta_{\text{vec},2}$ and $\beta_{\text{vec},3}$. The characteristic maximum in the state basis set plots originates from one two-level term while the marked decrease is due to a number of three-level contributions, each of opposite sign from the predominant two-level contribution. The two-level contribution can be expressed in terms of the familiar quantities f_{gn} (oscillator strength of a transition from g to n), $\hbar\omega_{gn}$ (energy difference between g and n), and $\Delta\mu_{gn}$ (difference in dipole moments between n and g). If the summation in eq 8 is limited to one dominant transition and the charge transfer is unidirectional, as is the case for typical organic chromophores, the classic two-level model originally proposed by Oudar is obtained (eq 11).⁶ Since each of the three design parameters in this approximation has a chemically-intuitive connection, Oudar's phenomenological model has been extensively utilized both in chromophore design and in rationalizing NLO properties.

$$\beta_{\text{Oudar}} = \frac{3e^2}{2} \frac{\hbar\omega_{gn} f \Delta\mu_{gn}}{[(\hbar\omega_{gn})^2 - (2\hbar\omega)^2][(\hbar\omega_{gn})^2 - (\hbar\omega)^2]} \quad (11)$$

In contrast to $\beta_{\text{vec},2}$, no analogous simplification for the non-negligible sum of three-level contributions is currently available. Since the $\beta_{\text{vec},3}$ expression includes excited state to excited state (i.e., two-photon) transition integrals ($r_{nn'}$), it is perhaps not unexpected that no three-level analogue of β_{Oudar} currently exists to simplify the three-level contributions to β_{vec} . Thus we cannot neglect the three-level contributions, nor can we express them in an intuitively appealing fashion.

As previously reported,¹⁸ the fundamental assumption (empirical) that permits a chemical interpretation of the NLO response presumes that the $\beta_{\text{vec},3}$ component is proportional to the $\beta_{\text{vec},2}$ components for a wide variety of molecular structures. Specifically, the three-level terms reduce β_{vec} by approximately half the value of $\beta_{\text{vec},2}$.¹⁸ We suggest, therefore, that a qualitative but instructive description of the NLO response can be obtained by analyzing the charge-transfer state(s) contributing to two-level terms of the quadratic hyperpolarizability, even though the $\beta_{\text{vec},3}$ contributions are non-negligible. We find that one excited state usually dominates the magnitude of $\beta_{\text{vec},2}$, and taken together, these two physically reasonable assumptions allow us to deduce the all-important rationalizations for the response of a given chromophore by simply analyzing the electronic properties of the influential excited state.

(Pyridine)M(CO)₅ Derivatives. Chemically-Oriented Description of β . To determine if the analytical paradigm discussed above applies to the (pyridine)M(CO)₅ chromophores, the relative two-level ($\beta_{\text{vec},2}$) and three-level contributions ($\beta_{\text{vec},3}$) of chromophores **8–15** were computed and are provided in Table 2. With the exception of the dimethylamino derivative (**15**), which exhibits a minuscule β_{vec} ($0.55 \times 10^{-30} \text{ cm}^5 \text{ esu}^{-1}$), the three-level

Scheme 1. Analysis of β for Molecule 9

two-level contribution ($\beta_{\text{vec},2}$)	-29.2
three-level contribution ($\beta_{\text{vec},3}$)	13.7
total ($\hbar\omega = 0.65 \text{ eV}$)	-15.5
β_{vec} in units of $10^{-30} \text{ cm}^5 \text{ esu}^{-1}$	

Assumption 1. Three-level terms scale as two-level terms. Therefore, understanding two-level terms will provide qualitative understanding of β .

73% of the total two-level contribution comes from one two-level term involving a MLCT at 401 nm with an oscillator strength of 0.21.

Assumption 2. The two-level contribution is dominated by one excited state. Therefore, understanding this excited state will provide qualitative understanding of β .

$$\Psi_{\text{ExcitedState}} = 0.97\Phi_{\text{HOMO} \rightarrow \text{LUMO}}$$

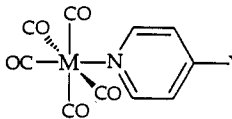
Assumption 3. The β -determining excited state transition is dominated by one transition between molecular orbital configurations as dictated by the ZINDO CI coefficients. A description of this transition leads to a chemical interpretation of β , and it is generally (for strong hyperpolarizabilities) the HOMO \rightarrow LUMO transition.

components are of opposite sign and roughly half of the two-level contributions for these chromophores, in adherence with the aforementioned guidelines regarding the relationship between $\beta_{\text{vec},2}$ and $\beta_{\text{vec},3}$. Using the formyl derivative (**9**) as an example (Scheme 1), β_{vec} ($-15.5 \times 10^{-30} \text{ cm}^5 \text{ esu}^{-1}$) is a sum of $\beta_{\text{vec},2}$ ($-29.2 \times 10^{-30} \text{ cm}^5 \text{ esu}^{-1}$) and $\beta_{\text{vec},3}$ ($13.7 \times 10^{-30} \text{ cm}^5 \text{ esu}^{-1}$). The anomalous dimethylamino derivative (good donor substituent) is calculated to possess a negligible hyperpolarizability, and the minute two-level and three-level contributions do not conform to our empirical model.

Scheme 1 enumerates the additional assumptions necessary for understanding the electronic origins of the NLO response in the prototype chromophore (**9**). Note that one optical transition (an MLCT excitation) is responsible for 73% of the second-order response within the SOS formalism. Thus, a qualitative explanation for β can be obtained by simply analyzing this important excited state, essentially reducing the NLO problem to an extension of the linear optical problem. This conclusion was found to be equally valid for the other metal-pyridine chromophores.

Experimental and calculational details concerning the pivotal charge-transfer transition (λ_{CT}) in molecules **8–17** are summarized in Table 4. Note that the computed transition energies for the $M = \text{Cr}$ complexes are in favorable agreement with experiment where $M = \text{W}$, typically within 20 nm of the observed spectral maximum. This accuracy has been noted previously,³⁴ and the present trends are not unexpected. Nevertheless, this level of agreement is crucial for the present study, since we are seeking to understand the NLO properties of (pyridine)tungsten pentacarbonyl complexes by examining (pyridine)chromium pentacarbonyl electronic structures. The optical absorption data listed in Table 4 are in accord with the observations of Wrighton and co-workers,³⁸ in that the MLCT transition energy is bathochromically shifted as the 4-pyridine substituent becomes a stronger electron acceptor. For example, λ_{CT} for $Y = \text{NO}_2$ (446 nm) $>$ $Y = \text{COH}$ (401 nm) $>$ $Y = \text{H}$ (354 nm) $>$ $Y = \text{NH}_2$ (335 nm). Clearly, the dispersive component of β_{Oudar} serves to enhance the NLO response as the acceptor strength of the substituted moiety increases. As shown in Table 4, the numerator components of the two-level model (f and $\Delta\mu$) also increase as Y becomes a stronger electron acceptor. Not surprisingly, the NLO susceptibilities (Table 2) follow the same qualitative trend as the three crucial two-level parameters (i.e., $Y = \text{NO}_2 >$ $Y = \text{COH} >$ $Y = \text{H} >$ $Y = \text{NH}_2$). For the $Y = \text{N}(\text{CH}_3)_2$ chromophore (**15**), two optical transitions contribute to the NLO response: one MLCT excitation at 333 nm and a ligand-to-ligand charge-transfer excitation at 177 nm. Since the contribution to β by the predominant MLCT transition is rather modest in this molecular structure, other optical transitions can contribute in a non-negligible fashion.

Table 4. Comparison of Experimental and ZINDO-Derived Spectroscopic Data for the Excitation (λ_{CT}) That Dictates the Second-Order Response for Pentacarbonyl Group 6 Pyridine Chromophores (Oscillator Strength (f), Dipole Moment Change ($\Delta\mu$), and Absorption Wavelength (λ) for the Transition are Provided.^{a,b} For Purposes of Comparison, Data for *p*-Nitroaniline (16) and 4-Amino-4'-nitrostilbene (17) are Included



Y	λ_{expt}^c	λ_{calc}	f_{calc}	$\Delta\mu_{\text{calc}}$	character of transition ^d
8 NO ₂		446	0.22	-19.0	MLCT
9 COH	420-440	401	0.21	-17.0	MLCT
10 COCH ₃	420-440	393	0.19	-16.9	MLCT
11 C ₆ H ₅	330-340	351	0.23	-14.1	MLCT
12 H	332	354	0.14	-14.2	MLCT
13 C ₄ H ₉	328	344	0.10	-10.4	MLCT
14 NH ₂	290	335	0.10	-7.1	MLCT
15 N(CH ₃) ₂		333	0.13	-6.8	MLCT
		177	0.52	8.9	D → A CT
16	365	317	0.48	11.9	D → A CT
17	402	375	1.19	14.9	D → A CT

^a All wavelength data are in nanometers and dipole moment data are in debyes. ^b Note that M = Cr for computed values and M = W for experimental data. ^c Spectroscopic data (in dioxane) for 9-14 are from ref 13 and for 16-17 are from ref 17. ^d MLCT denotes primarily metal-to-ligand charge-transfer transition; D → A CT denotes primarily donor-to-acceptor charge-transfer transition.

We also note that λ_{CT} in these chromophores is not necessarily λ_{max} as pointed out in previous studies.³⁸ Experimentally, the predominantly ligand-field (or $d \rightarrow d$) transitions have been assigned at lower energies than the MLCT bands for Y = donor chromophores; however, this ordering is reversed for the Y = acceptor ligands. Since the contribution to β by Laporte-forbidden ligand field transitions should be minor by virtue of modest f_{gn} and $\Delta\mu_{\text{gn}}$ values, spectral data for these transitions are omitted from Table 4.

In comparing the charge-transfer spectral data for *p*-nitroaniline (16) with those for the transition metal complexes, two important differences emerge. First, the oscillator strengths of the charge-transfer transitions in the transition-metal NC₅H₄Y complexes (Y = acceptor) are significantly lower than those for typical push-pull benzene chromophores. However, the corresponding $\Delta\mu$ and ω_{gn}^{-1} for the transitions are greater in the metal-based chromophores relative to *p*-nitroaniline. Thus, within the context of the two-level model, it appears that the energy and magnitude of charge transfer in these metal-containing molecules render them attractive candidates for molecular components of second-order materials; however, their modest oscillator strengths dictate that their second-order responses will only be comparable to, as opposed to significantly greater than, those of π -organic molecules of similar molecular dimensions. Our previous contribution on ferrocenyl and chromium arene chromophores concluded that some classes of organometallic chromophores fail to exhibit significant NLO responses due to a pseudocentrosymmetric environment about the metallic centers, and therefore MLCT transitions in these molecules possess characteristically small $\Delta\mu$ values.¹⁸ Clearly, the coordination compounds examined herein present a different situation in that relatively small oscillator strengths are now the limiting parameter.

To probe further the influential charge-transfer state in the pyridine chromophores and *p*-nitroaniline, the calculated changes in electronic charge density between ground state and excited state are displayed in Figure 3. In the (pyridine)Cr(CO)₅ molecule, 0.88 electrons are transferred from the metal fragment to the NC₅H₄ ring in the MLCT transition. Note that 0.56 of the donated electron density originates in the chromium d_{xz} orbital. The charge-transfer picture for (4-formylpyridine)Cr(CO)₅ is similar in that the metal fragment donates extensive electron

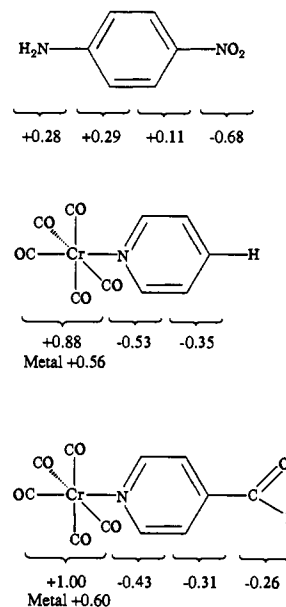


Figure 3. The difference in electronic populations between ground state and crucial excited state for two prototypical (pyridine)Cr(CO)₅ derivatives and a traditional organic chromophore as determined by ZINDO calculations. A negative population is indicative of an increase in electron density in the charge-transfer process.

density (1.00 electron) to the coordinated ligand. Surprisingly, the "acceptor substituent" (formyl group) receives only 0.26 of this electron, with the remaining density transferred to the pyridine ring. In contrast, the charge-transfer picture in *p*-nitroaniline is radically different. For the organic chromophore, only 0.68 electrons are transferred from the aminophenyl structure (donor) to the nitro acceptor. As discussed previously,^{18,28} a phenyl group adjacent to a donor, rather than the donor moiety itself, typically serves as the donor of electrons in π -to- π^* optical transitions in electronically acentric conjugated organic chromophores.

A molecular orbital description of β can be obtained by decomposing the MLCT excitation into transitions between molecular configurations (i.e., transitions between filled and unfilled molecular orbitals). As delineated in Scheme 1 (assumption 3), a HOMO → LUMO excitation is an excellent representation of the crucial MLCT in the representative formylpyridine chromophore 9. The simplified molecular orbital diagram of 9 (Figure 4) describes the frontier molecular orbital interactions between the Cr(CO)₅ and 4-formylpyridine moieties. In this diagram, the C_s symmetry of the molecule dictates that all σ orbitals (gerade symmetry) intermix as can all π orbitals (ungerade symmetry).

The electronic structural details of the C_{4v} M(CO)₅ fragment are well-established.⁴⁰ The fully occupied "pseudo- t_{2g} set" of metal d_x orbitals are split into a b_2 and e blocks,³⁸ with the e orbitals possessing the proper spatial characteristics to overlap with an attached ligand. In the case of chromophore 9, only one of these two e orbitals (d_{xz} in our labeling scheme) will interact with the pyridine π -network. Clearly, all three of these metal-based orbitals possess some amount of CO character; however, the orbitals will be drawn as purely metal orbitals for clarity. Of the "pseudo- e_g " set of metal d_o orbitals, only one will overlap with the σ system of the nitrogen-bound ligand, that being the d_{xz} orbital (unoccupied) in our coordinate system. The fragment orbitals of the 4-formylpyridine fragment are also straightforwardly understood. The π -symmetry LUMO is reminiscent of one of the degenerate LUMO pairs of benzene with a significant COH perturbation and will be labeled as a π^* orbital. Likewise,

(40) See, for example: Albright, T. A.; Burdett, J. K.; Whangbo, M. H. *Orbital Interactions in Chemistry*; Wiley: New York, 1985; Chapter 17.

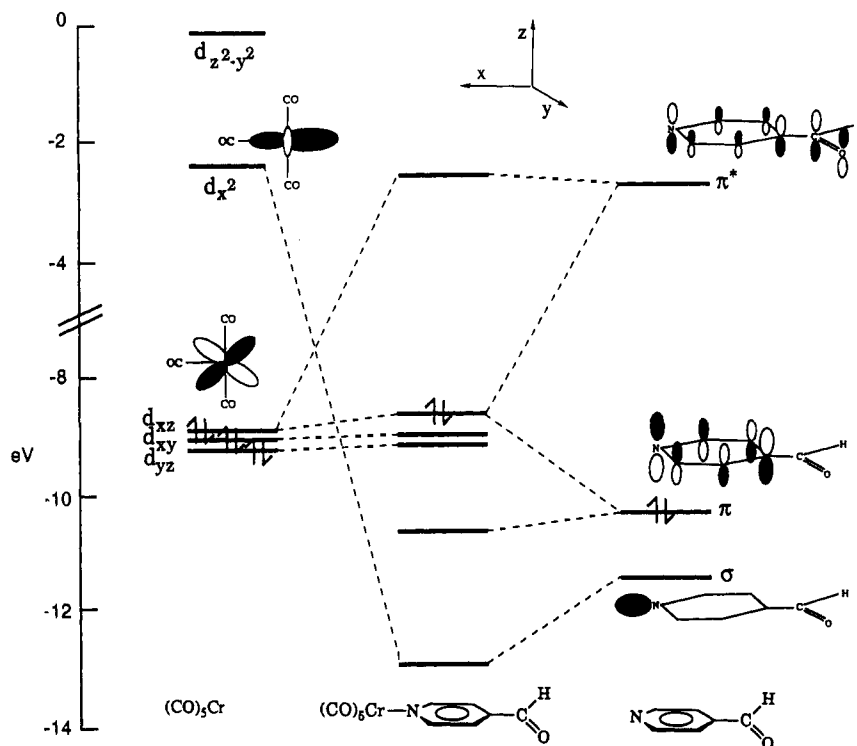


Figure 4. Molecular orbital diagram for the representative (pyridine)Cr(CO)₅ chromophore, **9**. The Cr(CO)₅ fragment labels represent the Cr orbitals that dominate a given Cr(CO)₅ fragment orbital.

Table 5. Comparison of ZINDO-Derived Molecular Orbital and SCF Fragment Orbital Energetics for Three Representative Pentacarbonyl(pyridine)chromium(0) Derivatives^a

Y	molecular orbital energy data			fragment orbital energy data ^b			λ_{CT}^{exp}
	ϵ_{HOMO}	ϵ_{LUMO}	$\Delta\epsilon_{HOMO \rightarrow LUMO}$	$\epsilon(Cr d_x)$	$\epsilon(py \pi^*)$	$\Delta\epsilon_{d_x \rightarrow \pi^*}$	
14 NH ₂	-7.91	-1.00	6.91	-8.11	-1.07	7.04	290 (4.27)
12 H	-8.07	-1.31	6.76	-8.22	-1.39	6.83	332 (3.73)
9 COH	-8.22	-2.12	6.10	-8.34	-2.15	6.19	420 (2.95)

^a All energy data are in units of electronvolts, except for the experimental λ_{CT} values, which are in both nanometers (ref 15) and electronvolts (in parentheses). ^b Cr d_x denotes the Cr(CO)₅ fragment orbital involved in π -bonding to the ligand, and py π^* denotes the pyridine fragment LUMO.

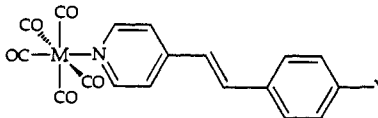
the HOMO is essentially identical to one of the HOMO pairs of benzene and will be labeled as a π orbital. Slightly lower in energy is the nitrogen lone-pair fragment orbital, which is directed toward the metal-based orbital of ungerade symmetry.

From the MO diagram in Figure 4, the primary molecular interaction involves the formation of a σ -linkage (coordinate covalent bond) between the nitrogen lone pair (σ) and the empty d_x metal-based orbital. The most striking feature of the MO diagram is the apparent lack of strong π -electron interactions between the two fragments. Note that the energetics of all π orbitals in both fragments are essentially unperturbed upon interaction. Specifically, the HOMO of the pyridine fragment interacts only weakly with the appropriate filled d_x metal orbital (d_{xz}) to raise its energy above that of the other two d_x orbitals, thereby forming the HOMO of the molecule. This molecular orbital is 93% d_{xz} , 5% pyridine π , and 1% pyridine π^* , displaying near-negligible covalent character. Since the π^* LUMO of the pyridine fragment does not strongly interact with any metal orbitals, it becomes the LUMO of the molecule ($\sim 94\%$ pyridine π^* and only $\sim 2\%$ metal d_{xz}). Due to poor π -coupling between interacting fragments, the HOMO of the molecule is predominantly metal fragment based and the molecular LUMO is primarily ligand based. The MLCT (represented by a HOMO \rightarrow LUMO excitation) therefore possesses only a modest oscillator

strength (small overlap between ground state and excited state) and involves significant charge transfer (promotion of an electron from a $\sim 93\%$ metal orbital into a $\sim 94\%$ ligand-based orbital).

Chemically-oriented structure-property relations for the other (Y-C₅H₄N)M(CO)₅ chromophores can be readily extrapolated from the MO diagram of the formyl derivative. Using a strategy similar to the one employed for organic chromophores,²⁸ NLO responses here can be qualitatively understood by examining the energetics of frontier molecular and frontier fragment orbitals. As shown in Table 5 for chromophores **9**, **12**, and **14**, the energy of the optical transition (λ_{CT})⁻¹, and therefore β , correlates well with the energetics of the molecular LUMO and of the ligand fragment LUMO in these complexes. For example, as Y becomes a stronger acceptor, the energy of the pyridine π^* orbital is decreased (-1.07 eV for Y = NH₂, -1.39 eV for Y = H, -2.15 eV for Y = COH). Since the molecular LUMO is largely π^* -centered, one expects (and finds) that the energetics of the LUMO are extremely sensitive to 4-position derivatization. As anticipated, neither the energy of the d_x fragment orbital nor the energy of the metal-based molecular HOMO is exceptionally sensitive to 4-position derivatization (-7.91 eV for Y = NH₂, -8.07 eV for Y = H, and -8.22 eV for Y = COH). Thus, the HOMO-LUMO gap is sensitive to derivatization and correlates well with observed trends in both λ_{CT} and β .

Table 6. Comparison of Experimental and ZINDO-Derived Molecular Hyperpolarizabilities^{a,b} (β_{vec}), Two-Level Contributions to the Response ($\beta_{\text{vec},2}$), and Three-Level Contributions ($\beta_{\text{vec},3}$) to the Response at 1.91 μm ($\hbar\omega = 0.65$ eV) for a Series of Group 6 Stilbazole Derivatives (For Purposes of Comparison, Data for *p*-Nitroaniline (16) and 4-Amino-4'-nitrostilbene (17) are Provided)



Y	$\beta_{\text{vec}}^{\text{expt } c}$	$\beta_{\text{vec}}^{\text{calc}}$	$\beta_{\text{vec},2}^{\text{calc}}$	$\beta_{\text{vec},3}^{\text{calc}}$	$\beta_{\text{vec}}^{\text{calc,corr } d}$
18 NO ₂	-20	-22.8	-99.4	76.6	-50
19 COH	-17	3.54	-44.7	48.2	-22
20 H	-5.7	7.91	-34.2	42.1	-17
6 N(CH ₃) ₂ ^e		34.7	28.4	6.3	14
6 N(CH ₃) ₂ ^f	61	65.5	39.6	25.9	20
16	9.2	10.7	17.2	-6.56	
17	40	46.4	106	-59.1	

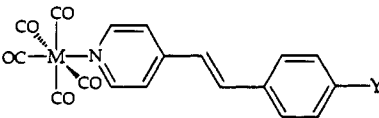
^a All NLO data are in units of 10^{-30} cm⁵ esu⁻¹. ^b Note that M = Cr for all computed responses and M = W for tabulated EFISH values. ^c NLO data for transition-metal chromophores 18–20 are from ref 15; organic chromophore data are from ref 17. ^d Defined as $\beta_{\text{vec},2}/2$. See text. ^e Computed response at 1.91 μm ($\hbar\omega = 0.65$ eV). ^f Computed response at 1.064 μm ($\hbar\omega = 1.17$ eV) for purposes of comparison with experimental value.

While the "NLO mechanism" in the (pyridine)M(CO)₅ chromophores is somewhat different from that for traditional organic chromophores, the origins of the second-order responses of the metal-based structures are not completely dissimilar from those found in carbon-based, electronically-acentric chromophores of similar molecular size. The ZINDO-SOS treatment unambiguously confirms the qualitative mechanism advanced previously by Cheng, Marder, and co-workers¹³ and has allowed detailed analysis of the origins. The obvious next step is to inquire concerning the effects of increasing the π -conjugation length between the metallic moiety and the acceptor, and to determine if, by analogy to organic systems, this modification increases the second-order response.

(Stilbazole)M(CO)₅ Derivatives. Nonlinear Optical Response. A recent publication¹⁵ reports the synthesis, characterization, and observed quadratic hyperpolarizability for three molecules of the type (4-acceptor-stilbazole)W(CO)₅, 18–20; Table 6. To further calibrate our ZINDO-SOS analysis, a model chromophore of the type (4-donor-stilbazole)W(CO)₅ (6), where donor = N(CH₃)₂, was also synthesized and characterized (eqs 6 and 7; Table 1; vide supra). The ZINDO-SOS-derived responses for all four group 6 pentacarbonyl stilbazole derivatives are compared in Table 6. Note that results for dimethylamino derivative 6 are distinctly different from those for the other three molecules. Specifically, the measured responses of chromophores 18–20 ($\hbar\omega = 0.65$ eV) are negative, as are their respective computed two-level contributions, while the measured response of anomalous chromophore 6 possesses a positive β ($\hbar\omega = 1.17$ eV) and a positive two-level contribution.

Before examining further the ZINDO results for transition-metal stilbazole derivatives, let us first examine experimental trends in the NLO and linear optical experimental data (Tables 1, 6, and 7). The β_{vec} of 4-amino-4'-nitrostilbene (40×10^{-30} cm⁵ esu⁻¹) exhibits a 4-fold enhancement relative to the lower conjugation length *p*-nitroaniline (9.2×10^{-30} cm⁵ esu⁻¹). A factor of 3–6 increase in β_{vec} in going from a disubstituted benzene to a disubstituted stilbene (keeping donor and acceptor moieties constant) is a well-established trend for π -organic chromophores.¹⁷ However, the $\beta_{\text{vec}}^{\text{expt}}$ values for the (4-formylpyridine)tungsten pentacarbonyl chromophore (Table 2, -12×10^{-30} cm⁵ esu⁻¹) and the stilbazole analogue (Table 6, -17×10^{-30} cm⁵ esu⁻¹) reveal only a modest increase in the second-order response with increased conjugation length, an increase far less than that typically observed for π -organic chromophores. Note that a

Table 7. Comparison of Experimental and ZINDO-Derived Spectroscopic Data for the Two Excitations That Dictate the Second-Order Response in Group 6 Stilbazole Chromophores (Oscillator Strengths (f), Dipole Moment Changes ($\Delta\mu$), and Absorption Wavelengths (λ) for Each Transition are Provided.^{a,b} For Purposes of Comparison, Data for *p*-Nitroaniline (16) and 4-Amino-4'-nitrostilbene (17) are Provided)



Y	optical transition 1				optical transition 2			
	$\lambda^{\text{expt } c}$	λ^{calc}	f^{calc}	$\Delta\mu^{\text{calc}}$	$\lambda^{\text{expt } c}$	λ^{calc}	f^{calc}	$\Delta\mu^{\text{calc}}$
18 NO ₂	425	389	0.66	-16.3	322	323	0.72	-7.12
19 COH	420	376	0.68	-12.3	320	315	0.68	1.54
20 H	390	371	0.69	-11.3	302	315	0.54	1.84
6 N(CH ₃) ₂	421	382	1.15	3.8				
16	365	317	0.48	11.9				
17	402	375	1.19	14.9				

^a All wavelength data are in nanometers and dipole moment data are in debyes. ^b Note that M = Cr for computed values and M = W for experimental data. ^c Spectroscopic data (in dioxane) for 18–20 are from ref 13, for 16–17 are from ref 17, and for 6 are from this work.

Scheme 2. Analysis of β for Molecule 19

two-level contribution ($\beta_{\text{vec},2}$)	-44.7
three-level contribution ($\beta_{\text{vec},3}$)	48.2
total ($\hbar\omega = 0.65$ eV)	3.54

Assumption 1. Three-level terms should scale as roughly $1/2$ the two-level terms. This is not strictly borne out by the computations, presumably due to inaccuracies in the geometrical input parameters. However, we assume $\beta_{\text{vec},3} \approx 1/2\beta_{\text{vec},2}$, thus generating a "corrected" value ($\beta_{\text{vec}}^{\text{calc,corr}}$) of -22×10^{-30} cm⁵ esu⁻¹. Understanding the adjusted two-level contributions will provide qualitative understanding of β .

99% of the total two-level contribution comes from one two-level term involving a MLCT at 376 nm with an oscillator strength of 0.68.

Assumption 2. The two-level contribution is dominated by one excited state. Therefore, understanding this excited state will provide qualitative understanding of β .

$$\Psi^{\text{ExcitedState}} = 0.92\Phi_{\text{HOMO}} \rightarrow \text{LUMO}$$

Assumption 3. The β -determining excited state transition is dominated by one transition between molecular orbital configurations as dictated by the ZINDO CI coefficients. A description of this transition leads to a chemical interpretation of β .

similar situation exists for the Y = H derivatives and, moreover, that the NLO response appears to be rather insensitive to derivatization of the styryl ring, in direct contrast to traditional π -organic architectures. Additionally, the experimental optical absorption data of Table 7 suggest that the energetics of the lowest-lying optical transition are also relatively insensitive to the derivatization of the chromophore. Specifically, upon replacement of NO₂ with an H substituent, λ_{CT} blue-shifts by only 35 nm in the (4-Y-styrylpyridine)W(CO)₅ complexes, while an optical shift of over 100 nm would be observed with the analogous substitution in a classical donor-acceptor stilbene system. The experimental data for this class of molecules thus suggest that the electronic origin of the optical nonlinearities is very different from that encountered in classical π -organic chromophore systems.

The ZINDO-SOS-derived quadratic hyperpolarizability data for the (4-Y-stilbazole)Cr(CO)₅ complexes are tabulated in Table 6. In direct contrast to nearly all molecules examined previously, the $\beta_{\text{vec},3}$ contributions for these particular chromophores rival and in some cases even surpass the $\beta_{\text{vec},2}$ contributions. As shown in Scheme 2 for the prototypical Y = COH chromophore, a sizable three-level component ($\beta_{\text{vec},3} = 48.2 \times 10^{-30}$ cm⁵ esu⁻¹) essentially

nullifies the two-level contribution ($\beta_{\text{vec},2} = -44.7 \times 10^{-30} \text{ cm}^5 \text{ esu}^{-1}$). As a consequence, the β_{vec} values do not agree with experiment for this class of chromophores. In addition, the computed data for the $Y = \text{N}(\text{CH}_3)_2$ molecule is also atypical, with $\beta_{\text{vec},2}$ ($28.4 \times 10^{-30} \text{ cm}^5 \text{ esu}^{-1}$) and $\beta_{\text{vec},3}$ ($6.3 \times 10^{-30} \text{ cm}^5 \text{ esu}^{-1}$) being of the same sign.

Table 7 provides the information necessary to deduce the origin of the significantly large three-level contributions. Note that the ZINDO-SOS absorption energies are in excellent agreement with those found experimentally for the second transition and in good agreement for the first MLCT. For example, the representative formyl chromophore **19** is computed to possess transitions at 376 and 315 nm, while transitions are observed at 420 and 320 nm. The (4-*Y*-stilbazole)Cr(CO)₅ chromophores possess two, as opposed to one, low-lying excitations of reasonable intensity. However, only the lower energy transition (optical transition 1) possesses significant charge-transfer character ($\Delta\mu = -12.3 \text{ D}$ for the prototype **19**) and makes a significant two-level contribution to β_{vec} . Optical transition 2, while not enlarging the two-level contribution by virtue of a small $\Delta\mu$ (1.54 D for **19**), strongly couples to the first transition through an r_{12} transition moment, resulting in a sizable three-level component. Mathematically, an $r_{g1}r_{12}r_{2g}$ three-level term (where 1 represents the first state and 2 the second state) can (formally) be substantial when both transitions 1 and 2 are allowed and a large r_{12} coupling element exists, as is true for this class of molecules.

In marked contrast to previous computations of second-order responses, the ZINDO-SOS results of Table 6 are atypical, due to the surprisingly large $\beta_{\text{vec},3}$ contributions. Of obvious interest is whether these results are genuine or an artifact of our computations. The ZINDO algorithm accurately reproduces the observed optical spectra and computes a substantial *negative* two-level contribution, which correlates well with the experimentally-determined negative quadratic hyperpolarizabilities. Clearly, the anomalously large $\beta_{\text{vec},3}$ values force the computed responses (β_{vec}) to be positive rather than negative (as observed experimentally) for molecules **19** and **20**. One additional consideration concerns the "stability" of the anomalously large three-level elements. Traditionally, the two-level and three-level responses have proven rather insensitive to alterations in molecular input geometry.²⁵ However, we find here that small variations in certain metrical input parameters of the (stilbazole)Cr(CO)₅ molecules produce dramatic variations in $\beta_{\text{vec},3}$. For example, lengthening the Cr–N bond by as little as 0.05 Å reduces the three-level contribution in the prototypical chromophore **19** by ~50% without greatly affecting $\beta_{\text{vec},2}$. This intrinsic geometrical sensitivity of the computed response, taken with the ability of ZINDO to reproduce optical spectra and the observed negative value of β , leads us to suggest that the anomalously large three-level contributions are, in this case, largely due to inaccuracies (in the absence of extensive crystallographic data) in the metrical input parameters for chromophores **6** and **18–20**.

As a consequence, we have chosen to define a new parameter for the four stilbazole chromophores, $\beta_{\text{vec}}^{\text{calc,corr}}$, which is defined to be exactly half the computed $\beta_{\text{vec},2}$ for a particular molecule, in accordance with our past experiences in computed NLO responses. This empirical correction allows circumvention of the aforementioned problematic $\beta_{\text{vec},3}$ contributions and permits a qualitative NLO analysis of these chromophores. As shown in Table 6, the $\beta_{\text{vec}}^{\text{calc,corr}}$ values for chromophores **6** and **18–20** are in reasonable agreement with the EFISH-derived responses, both in sign and in magnitude. The $\beta_{\text{vec}}^{\text{calc,corr}}$ values for **6** and **18–20** listed in Table 6 further suggest that the electronic origin of the second-order nonlinearity for the three (4-acceptor-stilbazole)M(CO)₅ compounds is substantially different from that found in (4-(dimethylamino)stilbazole)M(CO)₅, and therefore the interpretation of the NLO responses of these two classes will be discussed separately.

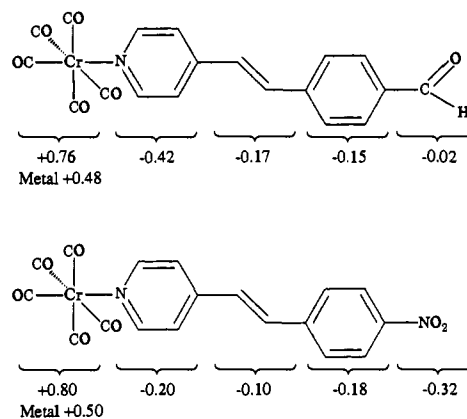


Figure 5. The difference in electronic populations between ground state and two crucial excited states for the prototypical (styrylpyridine)Cr(CO)₅ derivative (**19**) as determined by ZINDO calculations. A negative population reflects an increase in electron density in the charge-transfer process.

(4-Acceptor-4'-Stilbazole)M(CO)₅ Derivatives. Chemically-Oriented Description of β . As shown in Scheme 2, choosing to focus only on two-level contributions renders the analysis of the electronic origin of β in **19** relatively straightforward. One identifiable excited state (MLCT) comprises 99% of the total two-level contribution (optical transition 1, Table 7). Note that the computed spectral energies for this transition imply modest oscillator strength (small overlap between ground state and excited state) and involve significant charge transfer (promotion of an electron from a ~93% metal-based orbital into a ~94% ligand-based orbital).

The changes in electron density associated with the crucial optical excitation for two of these chromophores are shown in Figure 5. As anticipated, the metal serves as the source of electron density in the transition, and the excitation involves a substantial charge redistribution from metal fragment to ligand, as was found in the (pyridine)M(CO)₅ complexes above. Unexpectedly, however, the aromatic ring adjacent to the metal center serves as the primary acceptor of electron density and not the acceptor group itself. In the case of the 4-formylstilbazole chromophore, 0.42 electrons of the 0.76 electrons involved in the charge transfer migrates to the NC₅H₄ ring, and only 0.17 to the formyl group and the interposed arene π system. This situation is exacerbated in chromophores containing less potent electron acceptors, in that the pyridine ring is the primary acceptor. With the stronger NO₂ acceptor, more electron density is relocated at the nitro group; however, even in this molecule, 0.20 of 0.80 electrons involved in the MLCT process are transferred to the π -system of the pyridine ring. In other words, the seemingly innocent pyridine ring serves as an important acceptor group in this class of molecules. If the donor and acceptor were essentially equivalent, irrespective of the derivatization of the stilbazole ligand, this would explain the apparent insensitivity of λ_{CT} and β_{vec} to electronic characteristics of the acceptor substituent in the 4-position.

The simplified MO scheme displayed in Figure 6 provides additional evidence to support this hypothesis. As shown in Scheme 2, the HOMO \rightarrow LUMO excitation is a valid representation of the dominant MLCT. The molecular orbital diagram depicts the interaction of Cr(CO)₅ with the NC₅H₄C₂H₂C₆H₄-COH ligand. The overall bonding scheme is very similar to that for the 4-formylpyridine complex (Figure 4), with a few significant differences. The dominant covalent interaction involves the formation of a σ -linkage by mixing the occupied σ -ligand orbital with the unoccupied d_{z^2} Cr(CO)₅ orbital. The HOMO of the complex is metal based (~83% d_{z^2} , ~13% ligand π , ~11% ligand π_1^*), akin to the metal-centered HOMO in (4-formylpyridine)-Cr(CO)₅. The primary dissimilarity between the stilbazole and

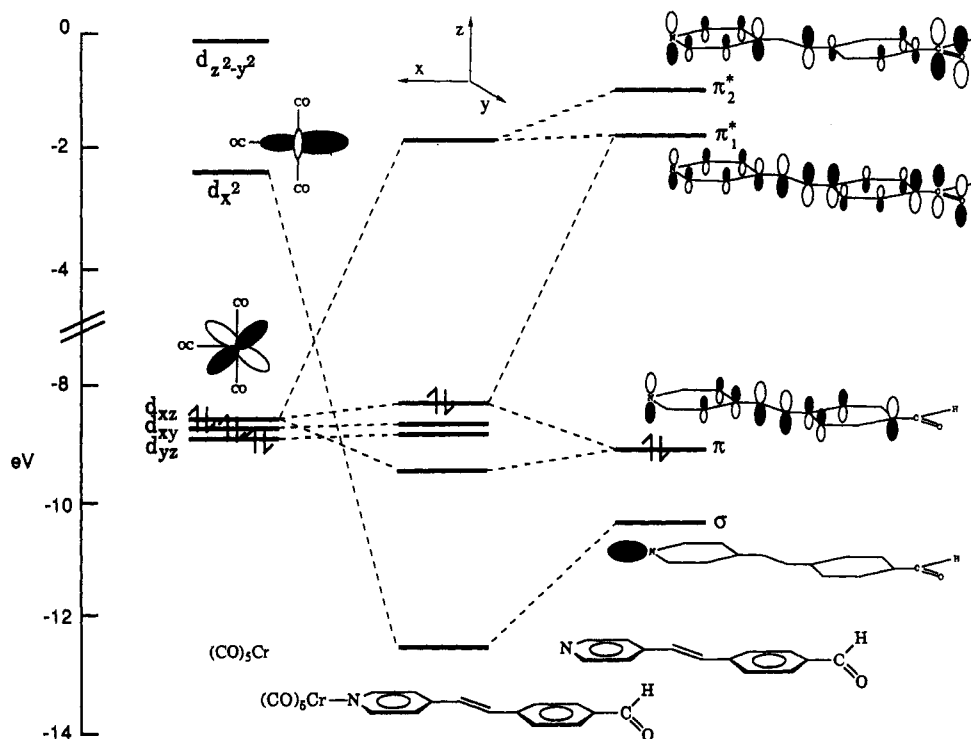
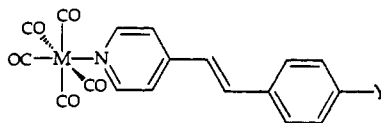


Figure 6. Molecular orbital diagram for the representative (styrylpyridine)Cr(CO)₅ derivative, **19**. The Cr(CO)₅ fragment labels represent the Cr orbitals that dominate a given Cr(CO)₅ fragment orbital.

Table 8. Comparison of ZINDO-Derived Molecular Orbital and SCF Fragment Orbital Energies for Four Representative Pentacarbonyl(stilbazole)chromium(0) Derivatives^a



Y	molecular orbital energy data			fragment orbital energy data ^b			λ_{CT}^{expt}	
	ϵ_{HOMO}	ϵ_{LUMO}	$\Delta\epsilon_{HOMO \rightarrow LUMO}$	$\epsilon(Cr d_x)$	$\epsilon(stpy \pi^*)$	$\Delta\epsilon_{d\pi \rightarrow \pi^*}$		
18	NO ₂	-8.07	-2.24	5.83	-8.26	-2.16	5.90	425 (2.91)
19	COH	-7.96	-1.86	6.10	-8.20	-1.76	6.44	420 (2.95)
20	H	-7.85	-1.57	6.28	-8.09	-1.53	6.56	390 (3.17)
6	N(CH ₃) ₂	-7.56	-1.40	6.16	-8.02	-1.37	6.65	421 (2.94)

^a All energy data are in units of electronvolts, except for the experimental λ_{CT} values, which are in both nanometers (**18–20**, ref 15) and electronvolts (in parentheses). ^b Cr d_x denotes the Cr(CO)₅ fragment orbital involved in π -bonding to the ligand, and stpy π^* denotes the stilbazole fragment LUMO.

the pyridine complexes is the involvement of two ligand π^* functions in the frontier orbital description in the former. These two orbitals, labelled π_1^* and π_2^* in Figure 6, contribute significantly to the molecular LUMO. Specifically, $\sim 70\%$ of the LUMO is π_1^* , $\sim 26\%$ is π_2^* , and less than $\sim 1\%$ is metal in character. From the orbital pictures in Figure 6, π_1^* is evenly distributed over all atomic centers, while π_2^* is localized on either end of the ligand. The ZINDO results show that the LUMO mixes these two functions, so as to constructively sum the pyridine density and destructively sum the formyl density. Qualitatively, the large positive charge induced on the pyridine ring, as a consequence of forming a coordinate covalent bond with an unoccupied metal orbital, lowers the energies of the two unoccupied ligand π^* orbitals, and in particular the π_2^* function, allowing the two antibonding π^* orbitals to interact to form a pyridine-based LUMO. In conclusion, the pyridine ring becomes the unexpected acceptor in these complexes due to the σ -accepting strength of the metal fragment.

The pyridine acceptor hypothesis can be further probed by comparing the fragment orbital energetics of (pyridine)Cr(CO)₅ and (4-formylpyridine)Cr(CO)₅ (Table 5) with those of the analogous styrylpyridine complexes (Table 8). In both classes of complexes, the energy of the metal-based HOMOs and the

primary contributor to the HOMOs (the metal-fragment d_{xz} function) are relatively insensitive to substituting a COH group for an H in the 4-position. In contrast, the molecular LUMOs are sensitive to derivatization, but they are much more sensitive in the pyridine complexes than in the stilbazole complexes. For example, the HOMO \rightarrow LUMO energy gap is 6.10 eV for (4-formyl-4'-stilbazole)Cr(CO)₅ and 6.28 eV for (4'-stilbazole)Cr(CO)₅, a difference of 0.18 eV. The difference in HOMO \rightarrow LUMO splitting for the analogous pyridine derivatives is much greater, 0.66 eV (6.10 eV for **9**, 6.76 eV for **12**). This translates into a significant blue-shifting of λ_{CT} (experimental) as COH is replaced with H in the pyridine complexes (88 nm), but only a small blue shift for the analogous structural variation in the stilbazole complexes (30 nm). The fragment orbital energetics of the influential fragment orbitals (metal d_x and ligand π^*) show a similar moderating effect upon changing from pyridine to stilbazole.

Perhaps the most striking counterintuitive effect discovered in this study is evidenced by comparative $\beta_{vec,2}$ data for push-pull α,ω -diphenylene polyenes and (η^1 -nitrogen ligand)Cr(CO)₅ structures of similar conjugation length shown in Table 9. Again, the $\beta_{vec,3}$ components of the computed response appear to be anomalously large for the metal carbonyl complexes and therefore

Table 9. Comparison of ZINDO-Derived Two-Level Contributions to the Molecular Hyperpolarizability^a ($\beta_{vec,2}$) for Formyl-Substituted Pyridine-Based Chromium Coordination Complexes and NH₂/NO₂ Derivatized α,ω -Diphenylene Polyene Molecules of Similar Dimensions at 1.91 μm ($\hbar\omega = 0.65 \text{ eV}$)

n	$\beta_{vec,2}^{calc}$	
0	-29.2	17.2
1	-44.6	105
2	-29.4	155
3	-22.1	221

^a All NLO data are in units of $10^{-30} \text{ cm}^5 \text{ esu}^{-1}$. ^b $n = 0$ row refers to $(\text{NC}_5\text{H}_4\text{COH})\text{Cr}(\text{CO})_5$ and $\text{H}_2\text{NC}_6\text{H}_4\text{NO}_2$.

are omitted from the tabulation. As anticipated, the $\beta_{vec,2}$ values for the amino-nitro push-pull derivatives dramatically increase as the π -bridge is lengthened ($105 \times 10^{-30} \text{ cm}^5 \text{ esu}^{-1}$ for $n = 1$, $155 \times 10^{-30} \text{ cm}^5 \text{ esu}^{-1}$ for $n = 2$, and $221 \times 10^{-30} \text{ cm}^5 \text{ esu}^{-1}$ for $n = 3$) in accord with common NLO chromophore design guidelines. However, note that the corresponding responses for the chromium pentacarbonyl derivatives *do not* display a dramatic increase with conjugation length. In fact, the computations predict that the response actually will decrease slightly with longer chain length. In all of these chromium chromophores, the pyridine ring is the primary acceptor, and this remains unchanged regardless of the length of the π -network. Therefore, the chromium chromophores would not be expected to display the conjugation length dependence of β_{vec} found in numerous organic systems.

In the previous contribution on organometallic molecules,¹⁸ we showed that η^5 -ferrocenyl and η^6 -chromium arene-based chromophores are very similar to π -organic molecules (i.e., increasing second-order response with increasing conjugation length) except that the charge-transfer character is only modest for ferrocenyl derivatives and small for the chromium systems due to the electronic pseudocentrosymmetry about the metal centers. One may wonder why the σ -withdrawing strength of the ferrocenyl and chromium tricarbonyl fragments is not an important factor in these chromophores, while such interactions appear to dictate the NLO response mechanism in the present pyridine complexes. The crucial difference between the two classes of molecules is that the ferrocenyl and chromium arene fragments are strongly coordinated to the π -ligand system through the metal π orbitals. The bonding in these molecules is significantly covalent, donors are strongly coupled to acceptors, and therefore π -organic chromophores serve as excellent models to these transition-metal chromophores. In contrast, for the pyridine structures examined herein, the primary interaction between metal and ligand is the formation of a coordinate covalent σ -linkage through metal σ orbitals, in which the π -network of the metal is poorly coupled to the ligand π -system. Molecules with coordinate covalent bonding and weakly coupled π -systems should display the effects of the metal as an inductive acceptor.⁴¹ Intermediate between the two extremes are metal carbene and

(41) To date, most researchers have constructed highly nonlinear chromophores by following the classical " π -donor linked to π -acceptor through a π -bridge" prescription. If, in fact, the inductive moiety mechanism is at work in these coordination complexes, equivalent organic σ -withdrawing substituents should also enhance the nonlinear susceptibility in π -organic networks. Electronegative fluorine atoms, for instance, could serve as inductive σ -acceptors. To illustrate the potential of employing organic inductive acceptors, the NLO responses for 4-amino-4'-fluorostilbene and 4-amino-2',3',4',5',6'-pentafluorostilbene were calculated to be 7.2×10^{-30} and $23.3 \times 10^{-30} \text{ cm}^5 \text{ esu}^{-1}$ respectively. Thus, replacing one hydrogen atom by a σ -accepting, π -donating fluorine atom has little effect upon β ; however, replacing all five hydrogen atoms by fluorine atoms dramatically enhances the NLO response. One can conclude from these data that, in a qualitative sense, the perfluorophenyl acceptor group is approximately half as potent as a 4-nitro substituent, since β for 4-amino-4'-nitrostilbene (17) is $46.4 \times 10^{-30} \text{ cm}^5 \text{ esu}^{-1}$. The calculations show that the excited state is completely devoid of fluorine character while the phenyl group attached to the fluorine atoms is the primary acceptor, indicative of an inductive mechanism.

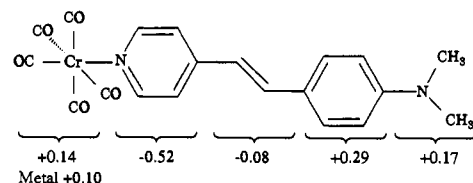


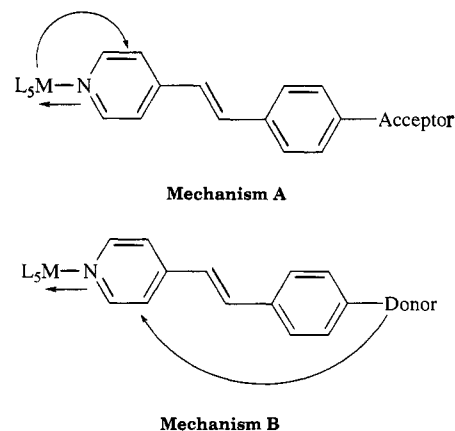
Figure 7. The difference in electronic populations between ground state and crucial excited state for (4-(dimethylamino)-4'-stilbazole) $\text{Cr}(\text{CO})_5$ (6) as determined by ZINDO calculations. A negative population reflects an increase in electron density in the charge-transfer process.

carbyne structures, and these results will be reported in a future contribution.

(4-Donor-4'-stilbazole) $\text{M}(\text{CO})_5$ Derivative. Chemically-Oriented Description of β . We now turn to the model (4-(dimethylamino)-4'-stilbazole) $\text{M}(\text{CO})_5$ chromophore (6), the synthesis and NLO response of which are reported above. This structure is found to possess a surprisingly large β_{vec}^{exp} , which is of opposite sign to the three other stilbazole structures (18–20) as shown in Tables 1 and 6. From a computational standpoint, the calculated β_{vec} at 1064 nm ($65.5 \times 10^{-30} \text{ cm}^5 \text{ esu}^{-1}$) is very close to the observed susceptibility ($61 \times 10^{-30} \text{ cm}^5 \text{ esu}^{-1}$). In order to more accurately compare the dimethylamino derivative to chromophores 18–20 measured at 1910 nm, β_{vec} at this lower energy was computed to be $34.7 \times 10^{-30} \text{ cm}^5 \text{ esu}^{-1}$. As was found for the other three stilbazole chromophores, the relative magnitudes of $\beta_{vec,2}$ and $\beta_{vec,3}$ do not adhere to the usual empirical model. Therefore, corrected NLO susceptibilities of 14×10^{-30} and $20 \times 10^{-30} \text{ cm}^5 \text{ esu}^{-1}$ were calculated for chromophore 6 at 1910 and 1064 nm, respectively.

Within the ZINDO-SOS model, $\beta_{vec,2}$ of 6 is dominated (>60%) by one excited state in the SOS formalism. Not surprisingly, this crucial charge-transfer transition is dominated (>90%) by an excitation from the molecular HOMO to the LUMO. Insight into the origin of the unusually large (and positive) response can be obtained from a description of the crucial charge-transfer transition (Figure 7). Note that the pyridine moiety serves as the primary acceptor in 6, while the dimethylamino moiety and adjacent aromatic ring are the primary donors. Thus the charge-transfer transition that dictates the NLO response is most accurately viewed as a *ligand-to-ligand excitation*, which is in the same direction as the ground state dipole moment, thereby explaining the positive value of β . Note that the predominant excitation also contains a metal \rightarrow pyridine charge-transfer component as shown in Figure 7, but it is of secondary importance since only ~ 0.14 electron $\text{M}(\text{CO})_5$ migrates toward the pyridinyl ring in the transition, compared to ~ 0.46 electron emanating from the opposite end of the structure.

As was found for chromophores 18–20, the major role of the metal fragment in 6 is that of an inductive acceptor. Rather than a MLCT resulting in a negative first hyperpolarizability (mechanism A), a LLCT transition now dominates β (mechanism B).



While the second-order susceptibility of **6** is unexpectedly large, it is still somewhat modest when compared with organic structures of similar size. The obvious next step in this research would be to increase the oxidizing strength of the weakly-coupled metal fragment to enhance the ligand-to-ligand charge transfer, which could potentially lead to metal-based chromophores that might compete with conventional push-pull π -organic architectures.⁴²

Conclusions

Several conclusions concerning the potential viability of using metal fragments weakly bound to π -electron networks as NLO chromophores have emerged from the present ZINDO-SOS computational study. Specifically:

(1) The computed linear and NLO properties of (pyridine)M(CO)₅ chromophores are in excellent agreement with experiment. The second-order response is largest for this class of complexes when electron-withdrawing groups are attached to the pyridine ring. Responses can equal and in some cases surpass those observed for optimal organic chromophores of similar molecular dimensions.

(2) The nonlinear susceptibilities of the pyridine-coordinated complexes are significantly enhanced relative to the free ligands, especially when electron acceptors are incorporated into the pyridine π -system.

(3) A low-lying MLCT transition is responsible for the NLO response of the pyridine complexes within the SOS formalism. This excitation possesses a large $\Delta\mu_{gn}$ and a relatively low ΔE_{gn} .

(42) As this paper was being prepared, a preliminary experimental finding that supports the conclusions discussed herein was communicated to us. Results from A. Pulham and R. G. Denny (private communication) determined that, in the class of complexes *cis*-RuCl₂(CO)₂(4-Y-4'-stilbazole)₂, the largest macroscopic second-order response ($\chi^{(2)}$) was found to be for Y = donor rather than Y = acceptor. Our preliminary computations indicate that the Ru²⁺ center is acting as an inductive acceptor, and therefore β would be expected to be largest when Y = donor.

However, the β_{vcc} -limiting factor is the intrinsically small oscillator strength associated with these MLCT excitations. The small oscillator strengths are due to the relatively poor π -coupling between metal and ligand as demonstrated by molecular orbital arguments.

(4) The agreement between computed and EFISH-determined second-order responses for (stilbazole)M(CO)₅ chromophores is somewhat less favorable. The source of the discrepancy is anomalously large three-level contributions to the responsivity, apparently reflecting slight inaccuracies in the chosen input geometries.

(5) The pyridine ring serves as a potent accepting group in the stilbazole complexes, due to an inductive interaction between metal and ligand. Since the charge-transfer transition is essentially invariant to derivatization at the stilbazole 4-position, both β and λ_{CT} are insensitive to derivatization.

(6) It is seen that weakly bound transition metal π -complexes do not display the dramatic increases in β_{vcc} with conjugation length observed for traditional organic chromophores.

(7) The inductive strength of the metal fragment must be considered in chromophoric coordination complexes where metal and ligand π -systems are weakly coupled. Currently unrealized molecular structures are under investigation that would exploit the inductive accepting properties of a metal fragment for β enhancement.

Acknowledgment. This research was supported by the NSF-MRL Program through the Materials Research Center of Northwestern University (Grant DMR9120521) and by the Air Force Office of Scientific Research (Contract 93-1-0114). P.A.L. thanks CNRS for a postdoctoral fellowship. We also thank Professor M. Zerner for graciously supplying us with the ZINDO program, Professor G. K. Wong for access to the EFISH equipment, and Mr. W. Lin for experimental assistance.